

## 9. GEOCHEMICAL EXPRESSION OF EARLY DIAGENESIS IN MIDDLE EOCENE-LOWER OLIGOCENE PELAGIC SEDIMENTS IN THE SOUTHERN LABRADOR SEA, SITE 647, ODP LEG 105<sup>1</sup>

M. A. Arthur,<sup>2</sup> W. E. Dean,<sup>3</sup> J. C. Zachos,<sup>2</sup> M. Kaminski,<sup>4</sup> S. Hagerty Rieg,<sup>2</sup> and K. Elmstrom<sup>2</sup>

### ABSTRACT

Geochemical analyses of the middle Eocene through lower Oligocene lithologic Unit IIIC (260–518 meters below seafloor [mbsf]) indicate a relatively constant geochemical composition of the detrital fraction throughout this depositional interval at Ocean Drilling Program (ODP) Site 647 in the southern Labrador Sea. The main variability occurs in redox-sensitive elements (e.g., iron, manganese, and phosphorus), which may be related to early diagenetic mobility in anaerobic pore waters during bacterial decomposition of organic matter. Initial preservation of organic matter was mediated by high sedimentation rates (36 m/m.y.). High iron (Fe) and manganese (Mn) contents are associated with carbonate concretions of siderite, manganoisiderite, and rhodochrosite. These concretions probably formed in response to elevated pore-water alkalinity and total dissolved carbon dioxide ( $\text{CO}_2$ ) concentrations resulting from bacterial sulfate reduction, as indicated by nodule stable-isotope compositions and pore-water geochemistry. These nodules differ from those found in upper Cenozoic hemipelagic sequences in that they are not associated with methanogenesis. Phosphate minerals (carbonate-fluorapatite) precipitated in some intervals, probably as the result of desorption of phosphorus from iron and manganese during reduction.

The bulk chemical composition of the sediments differs little from that of North Atlantic Quaternary abyssal red clays, but may contain a minor hydrothermal component. The silicon/aluminum (Si/Al) ratio, however, is high and variable and probably reflects original variations in biogenic opal, much of which is now altered to smectite and/or opal CT. An increase in the sodium/potassium (Na/K) ratio in the upper Eocene corresponds to the beginning of coarser-grained feldspar flux to the site, possibly marking the onset of more vigorous deep currents.

Although the Site 647 cores provide a nearly complete high-resolution, high-latitude Eocene-Oligocene record, the high sedimentation rate and somewhat unusual diagenetic conditions have led to variable alteration of benthic foraminifers and fine-fraction carbonate and have overprinted the original stable-isotope records. Planktonic foraminifers are less altered, but on the whole, there is little chance of sorting out the nature and timing of environmental change on the basis of our stable-isotope analyses.

### INTRODUCTION

A total of 117 samples of predominantly grayish-green, middle Eocene through lower Oligocene, nannofossil claystone and clayey nannofossil chalk from lithologic Unit IIIC (260–518 mbsf; Cores 105-647A-28R through -54R) in Hole 647A were collected for inorganic geochemical and stable isotopic analyses. The samples were collected initially for the following purposes:

1. To document possible changes in the geochemical composition of sediments and stable isotopic compositions of calcareous biogenic components in response to changes in paleoclimate and ocean circulation during the late Eocene to early Oligocene at high northern latitudes.
2. To document the composition of unusual authigenic nodules and/or beds in lithologic Unit IIIC.

The generally good core recovery, an apparently complete Eocene/Oligocene transition, and seemingly good (visual) preservation of calcareous microfossils led us to believe that our results would have a bearing on interpretation of climate and circulation

events that occurred in latest Eocene to earliest Oligocene time. However, as shown below, the most significant application for our geochemical and isotopic data is in the documentation of a rather unusual early diagenetic regime.

### METHODS

Samples were freeze-dried and ground to pass through a 100-mesh (149  $\mu\text{m}$ ) sieve. Splits of all samples were analyzed coulometrically (Huffman, 1985) for carbonate and total carbon (precision better than 1%) at the University of Rhode Island (URI). In addition, splits of many samples were sieved and selected for planktonic and benthic foraminifers for stable isotope studies. Splits of the ground samples were analyzed at the U.S. Geological Survey (USGS), Denver, for 10 major and minor elements by X-ray fluorescence (XRF) and 30 major, minor, and trace elements by induction-coupled, argon-plasma emission spectrometry (ICP) (Baedecker, 1987). Nine elements (aluminum, iron, magnesium, calcium, sodium, potassium, titanium, phosphorus, and manganese) were analyzed by both XRF and ICP, with essentially identical results between the two methods. Five samples contained concentrations of iron (Fe) and manganese (Mn) that were sufficiently high to cause interferences with XRF; hence, no XRF results are available for these samples. Analytical results are given in Table 1 and plotted vs. depth in Figures 1 through 6. The geochemical data have not been corrected for contribution of pore-water salts because porosities are typically lower than 40%. Sodium (Na) and magnesium (Mg) concentrations would be the main elements affected.

Carbonate components were analyzed for carbon and oxygen-isotope compositions at URI. Samples were ground to <50  $\mu\text{m}$ , roasted *in vacuo* at 390°C for 1 hr and reacted online in purified phosphoric acid at 50°C. The resulting  $\text{CO}_2$  gas was purified and introduced into a VG Micromass 602D mass spectrometer for analysis. Results are expressed in the standard delta notation relative to the PDB standard, where

$$\delta = (\text{Rsamp} - \text{Rstd}) \times 1000 \text{ Rstd},$$

and analytical precision was 0.1% for  $\delta^{18}\text{O}$  and 0.05% for  $\delta^{13}\text{C}$ .

<sup>1</sup> Srivastava, S. P., Arthur, M., Clement, B., et al., 1989. *Proc. ODP, Sci. Results*, 105: College Station, TX (Ocean Drilling Program).

<sup>2</sup> Graduate School of Oceanography, University of Rhode Island, Narragansett, RI 02882.

<sup>3</sup> U.S. Geological Survey, Box 25046, MS 939, Federal Center, Denver, CO 80225.

<sup>4</sup> Woods Hole Oceanographic Institution, Woods Hole, MA 02543. Now at Centre for Marine Geology, Dalhousie University, Halifax, Nova Scotia B3H, Canada.

**Table 1.** Geochemical analyses of samples from lithologic Unit IIIC, Hole 647A.

Sample	Core	Section	Interval	Depth (m)	SiO <sub>2</sub> -xrf (%)	Al <sub>2</sub> O <sub>3</sub> -xrf (%)	Al <sub>2</sub> O <sub>3</sub> -icp (%)	Fe <sub>2</sub> O <sub>3</sub> -xrf (%)	Fe <sub>2</sub> O <sub>3</sub> -icp (%)	MgO-xrf (%)	MgO-icp (%)	CaO-xrf (%)	CaO-icp (%)	Na <sub>2</sub> O-xrf (%)	Na <sub>2</sub> O-icp (%)	K <sub>2</sub> O-xrf (%)	K <sub>2</sub> O-icp (%)
281089	28.00	1.00	89.00	260.99	40.80	10.40	10.96	4.88	4.86	1.93	1.99	18.60	16.80	1.51	1.62	1.55	1.80
282052	28.00	2.00	52.00	262.12	36.70	8.57	9.26	5.69	5.72	1.78	1.83	21.20	19.60	1.35	1.62	1.43	1.92
283054	28.00	3.00	54.00	263.65	28.80	7.79	8.50	3.32	3.29	1.50	1.56	28.90	26.60	1.24	1.48	0.49	1.20
284068	28.00	4.00	68.00	265.28	49.60	11.80	12.47	4.84	4.72	2.14	2.16	11.90	11.34	1.84	1.89	1.62	1.68
301051	30.00	1.00	51.00	279.93	26.60	7.51	8.12	6.93	6.86	1.85	1.83	23.40	22.40	1.16	1.31	0.62	1.19
302092	30.00	2.00	92.00	281.82	33.20	9.10	9.82	3.71	3.72	1.59	1.61	24.60	23.80	1.42	1.62	0.99	1.44
303045	30.00	3.00	45.00	282.85	29.00	7.94	8.69	3.03	3.00	1.43	1.46	29.20	28.00	1.24	1.35	0.61	1.32
304098	30.00	4.00	98.00	284.88	36.30	9.84	10.39	3.81	3.58	1.66	1.66	23.10	22.40	1.40	1.48	1.19	1.56
305112	30.00	5.00	112.00	286.52	38.50	10.50	11.15	4.09	3.86	1.82	1.83	20.80	19.60	1.48	1.48	1.35	1.56
306097	30.00	6.00	97.00	287.87	36.10	9.92	10.58	3.83	3.58	1.67	1.66	22.50	21.00	1.32	1.48	1.13	1.44
307029	30.00	7.00	29.00	288.69	42.90	11.90	12.66	4.39	4.29	2.00	1.99	16.50	15.40	1.55	1.62	1.67	1.92
311029	31.00	1.00	29.00	289.29	39.20	10.50	11.33	4.30	4.29	1.79	1.83	20.30	19.60	1.40	1.62	1.25	1.56
312102	31.00	2.00	102.00	291.51	37.70	9.28	10.01	5.20	5.15	1.77	1.83	20.00	18.20	1.29	1.48	1.20	1.32
321049	32.00	1.00	49.00	299.09	36.00	7.97	8.69	3.43	3.43	1.45	1.49	25.20	23.80	1.31	1.48	0.96	1.20
322032	32.00	2.00	32.00	300.42	43.50	7.75	8.31	3.35	3.43	1.37	1.39	20.90	19.60	1.26	1.35	1.05	1.14
332018	33.00	2.00	18.00	309.98	36.00	8.88	9.45	4.11	4.15	1.59	1.64	23.40	22.40	1.31	1.48	0.97	1.32
351028	35.00	1.00	28.00	327.88	44.40	11.40	12.09	4.57	4.29	1.87	1.83	16.20	15.40	1.48	1.48	1.65	1.80
352029	35.00	2.00	29.00	329.39	43.90	11.30	11.90	4.58	4.29	1.83	1.83	17.10	16.80	1.39	1.48	1.55	1.68
353024	35.00	3.00	24.00	332.63	43.90	11.30	11.90	4.33	4.15	1.82	1.83	17.00	16.80	1.38	1.48	1.65	1.80
361068	36.00	1.00	68.00	337.88	43.00	10.70	11.15	4.67	4.43	1.80	1.83	17.10	16.80	1.40	1.62	1.53	1.68
362068	36.00	2.00	68.00	339.38	45.10	11.20	12.09	5.00	5.01	1.84	1.83	15.40	14.00	1.39	1.48	1.59	1.80
363068	36.00	3.00	68.00	340.88	42.90	10.40	11.15	6.74	6.72	1.71	1.66	15.00	14.00	1.24	1.35	1.59	1.68
364041	36.00	4.00	42.00	342.13	—	—	3.02	—	31.46	—	3.98	—	9.24	—	0.57	—	0.42
364068	36.00	4.00	68.00	342.38	44.20	11.10	11.52	4.70	4.58	1.82	1.83	16.10	15.40	1.37	1.48	1.60	1.68
372014	37.00	2.00	15.00	348.35	42.90	10.50	11.15	4.32	4.29	1.74	1.83	17.90	16.80	1.35	1.48	1.46	1.56
373015	37.00	3.00	15.00	349.85	40.70	10.30	10.96	4.18	4.15	1.66	1.66	19.70	18.20	1.21	1.29	1.41	1.56
374015	37.00	4.00	15.00	351.35	40.10	9.36	10.01	4.18	4.00	1.54	1.58	20.90	19.60	1.23	1.35	1.29	1.56
381036	38.00	1.00	36.00	356.76	38.00	8.72	9.26	4.02	3.86	1.43	1.44	23.10	22.40	1.24	1.29	1.13	1.44
382040	38.00	2.00	39.00	358.30	43.60	10.20	10.77	4.35	4.15	1.64	1.63	18.10	16.80	1.31	1.35	1.48	1.56
383041	38.00	3.00	41.00	359.81	44.30	10.00	10.58	4.31	4.29	1.57	1.63	17.90	16.80	1.34	1.35	1.49	1.68
384041	38.00	4.00	41.00	361.31	39.40	8.90	9.45	4.01	4.00	1.47	1.49	21.70	21.00	1.08	1.31	1.18	1.44
385041	38.00	5.00	41.00	362.81	47.40	10.80	11.52	4.77	4.72	1.74	1.83	14.90	14.00	1.33	1.48	1.58	1.68
386066	38.00	6.00	67.00	364.56	—	—	2.27	—	31.46	—	3.98	—	9.66	—	0.57	—	0.32
391017	39.00	1.00	17.00	366.27	53.90	12.10	12.47	5.08	5.01	1.92	1.99	9.57	9.24	1.54	1.62	1.83	1.92
392017	39.00	2.00	17.00	367.77	46.60	10.50	11.15	4.96	4.86	1.67	1.66	15.70	15.40	1.29	1.35	1.60	1.68
393019	39.00	3.00	19.00	369.29	45.80	10.30	10.96	4.37	4.29	1.65	1.66	16.10	15.40	1.33	1.35	1.52	1.68
411030	41.00	1.00	30.00	385.70	34.70	8.66	9.07	10.50	9.87	2.07	2.16	16.40	15.40	1.14	1.17	1.20	1.44
412030	41.00	2.00	30.00	387.20	37.10	9.44	10.01	3.80	3.58	1.45	1.46	23.60	22.40	1.14	1.19	1.22	1.44
413030	41.00	3.00	30.00	388.70	36.20	9.34	9.82	3.77	3.58	1.42	1.43	24.00	22.40	1.20	1.24	1.25	1.44
414030	41.00	4.00	30.00	390.20	40.60	10.60	11.33	4.21	4.15	1.60	1.64	20.00	19.60	1.25	1.35	1.66	1.92
415030	41.00	5.00	30.00	391.70	27.50	7.12	7.74	13.40	13.44	2.03	2.16	17.30	16.80	0.97	1.06	1.11	1.44
416070	41.00	6.00	70.00	393.60	21.60	6.10	6.61	16.60	17.16	2.27	2.32	17.20	16.80	0.82	0.96	0.59	1.09
421042	42.00	1.00	42.00	395.52	37.50	10.50	11.33	3.77	3.72	1.52	1.53	22.00	21.00	1.13	1.24	1.63	1.80
422048	42.00	2.00	48.00	397.07	34.70	9.81	10.39	4.33	4.29	1.41	1.41	23.40	22.40	1.08	1.16	1.55	1.92
424014	42.00	4.00	14.00	399.74	33.60	9.38	10.20	4.87	4.86	1.37	1.39	24.20	22.40	1.02	1.15	1.54	1.92
425028	42.00	5.00	28.00	401.38	27.60	7.61	8.31	4.64	4.72	1.20	1.21	29.30	28.00	0.96	1.05	1.06	1.68
426047	42.00	6.00	47.00	403.07	30.90	8.80	9.45	3.76	3.86	1.27	1.29	27.30	25.20	0.97	1.06	1.15	1.68
427049	42.00	7.00	49.00	404.59	31.90	8.78	9.45	4.14	4.00	1.28	1.33	26.40	25.20	1.05	1.13	1.25	1.80
431086	43.00	1.00	86.00	405.66	36.00	9.87	10.39	4.79	4.58	1.50	1.51	22.70	21.00	1.32	1.29	1.50	1.92
432029	43.00	2.00	29.00	406.59	38.20	10.70	11.33	4.29	4.00	1.56	1.54	21.00	19.60	1.25	1.24	1.59	1.80
433083	43.00	3.00	83.00	408.63	43.80	11.20	11.90	7.01	6.86	1.79	1.83	14.50	13.58	1.30	1.33	2.13	2.28
434025	43.00	4.00	25.00	409.55	21.20	5.59	6.23	4.31	4.43	1.16	1.21	31.30	29.40	1.17	1.35	0.81	1.06
435018	43.00	5.00	18.00	410.98	34.30	8.95	9.63	5.58	5.58	1.60	1.61	22.10	21.00	1.05	1.19	1.29	1.44
436027	43.00	6.00	27.00	412.57	47.40	12.40	12.85	6.52	6.43	1.94	1.99	12.10	11.62	1.34	1.35	2.22	2.40
437026	43.00	7.00	26.00	414.06	46.60	12.60	13.22	4.76	4.72	1.84	1.83	13.30	12.74	1.34	1.35	1.96	2.04
441080	44.00	1.00	80.00	415.30	41.10	10.90	11.71	4.73	4.72	1.66	1.66	18.70	18.20	1.28	1.35	1.55	1.80
442082	44.00	2.00	82.00	416.82	43.00	11.50	12.47	4.45	4.29	1.67	1.83	17.50	16.80	1.32	1.35	1.74	1.92

443087	44.00	3.00	87.00	418.36	38.20	10.60	11.15	4.02	3.72	1.56	1.56	21.80	19.60	1.24	1.20	1.67	1.92
444116	44.00	4.00	116.00	420.16	33.50	9.33	10.01	3.43	3.43	1.31	1.36	25.60	23.80	1.03	1.11	1.33	1.80
445074	44.00	5.00	74.00	421.24	29.10	8.06	8.69	3.00	2.86	1.17	1.16	29.90	28.00	0.97	1.04	0.72	1.44
446064	44.00	6.00	64.00	422.64	33.90	9.23	10.01	3.52	3.58	1.34	1.36	25.40	23.80	1.06	1.13	1.06	1.44
451102	45.00	1.00	102.00	425.11	39.80	10.20	10.96	4.39	4.29	1.55	1.56	20.50	19.60	1.15	1.24	1.56	1.68
453055	45.00	3.00	55.00	427.65	38.50	9.63	10.39	4.04	4.00	1.45	1.46	22.30	21.00	0.96	1.12	1.28	1.68
461047	46.00	1.00	47.00	434.27	47.70	11.10	11.71	5.35	5.29	1.76	1.83	14.00	13.30	1.27	1.35	1.59	1.68
462041	46.00	2.00	41.00	435.71	42.70	10.20	10.96	4.26	4.29	1.57	1.64	19.10	18.20	1.28	1.35	1.44	1.56
463041	46.00	3.00	41.00	437.21	46.40	11.50	11.90	5.61	5.29	1.78	1.83	13.80	13.16	1.36	1.32	1.68	1.80
464041	46.00	4.00	41.00	438.71	52.40	13.00	13.60	5.40	5.01	1.95	1.99	9.94	9.52	1.42	1.48	1.85	1.92
465057	46.00	5.00	57.00	440.37	47.00	11.80	12.28	6.48	6.01	1.89	1.83	13.30	12.74	1.31	1.48	1.74	1.92
465111	46.00	5.00	111.00	440.91	29.40	7.52	8.31	3.46	3.29	1.27	1.26	28.10	26.60	1.40	1.62	0.91	1.12
466057	46.00	6.00	57.00	441.87	46.50	11.70	12.28	5.29	5.15	1.76	1.83	14.20	13.30	1.37	1.35	1.65	1.80
471033	47.00	1.00	33.00	443.82	46.70	11.20	11.90	7.27	7.29	1.88	1.99	13.10	12.46	1.30	1.35	1.98	2.16
473016	47.00	3.00	16.00	446.66	49.00	12.50	13.03	5.30	5.15	1.88	1.83	12.20	11.48	1.32	1.35	1.75	1.80
474021	47.00	4.00	21.00	448.21	45.00	11.20	11.90	7.16	7.01	1.85	1.83	13.70	13.02	1.29	1.33	1.57	1.68
475021	47.00	5.00	21.00	449.71	39.10	9.56	10.20	4.61	4.58	1.52	1.54	21.20	19.60	1.18	1.25	1.41	1.56
476025	47.00	6.00	25.00	451.25	59.00	14.30	13.60	9.30	8.87	2.30	2.16	0.97	0.94	1.33	1.27	3.39	3.24
481007	48.00	1.00	7.00	453.27	—	3.21	3.21	—	37.18	—	3.65	—	6.16	—	0.39	—	0.58
481030	48.00	1.00	30.00	453.50	50.00	11.90	12.47	9.20	8.72	2.11	2.16	9.24	8.96	1.51	1.48	2.38	2.52
482034	48.00	2.00	34.00	455.04	40.80	9.97	10.58	4.36	4.15	1.62	1.61	20.40	19.60	1.29	1.28	1.32	1.44
483029	48.00	3.00	29.00	456.49	52.80	11.30	11.71	6.09	5.72	1.88	1.83	10.60	10.22	1.34	1.35	1.71	1.80
484032	48.00	4.00	32.00	458.02	48.90	11.30	12.09	4.68	4.58	1.79	1.83	13.70	12.88	1.15	1.28	1.53	1.68
485030	48.00	5.00	30.00	459.50	58.30	12.50	12.85	5.70	5.43	2.03	1.99	6.34	6.02	1.43	1.35	1.76	1.80
491074	49.00	1.00	74.00	463.54	47.40	11.40	12.09	4.66	4.58	1.94	1.99	14.20	13.44	1.31	1.48	1.55	1.68
492066	49.00	2.00	66.00	464.96	48.20	11.30	11.90	4.71	4.72	1.87	1.83	13.80	13.30	1.34	1.35	1.52	1.68
493080	49.00	3.00	80.00	466.60	33.40	7.80	8.31	8.23	8.01	2.09	2.16	17.30	16.80	1.07	1.23	0.95	1.20
494039	49.00	4.00	39.00	467.69	37.60	8.81	9.45	5.81	5.72	1.75	1.83	18.80	18.20	1.16	1.28	1.27	1.44
496043	49.00	6.00	43.00	470.73	40.60	7.97	8.69	3.48	3.43	1.36	1.43	22.60	22.40	1.16	1.16	1.05	1.20
501056	50.00	1.00	56.00	473.06	43.70	10.10	10.58	4.75	4.43	1.80	1.83	17.10	16.80	1.19	1.29	1.44	1.56
502056	50.00	2.00	56.00	474.56	45.20	10.50	11.15	5.29	4.86	1.84	1.83	15.60	15.40	1.09	1.31	1.60	1.68
503036	50.00	3.00	36.00	475.86	46.30	11.00	11.52	4.59	4.29	1.82	1.83	15.60	15.40	1.24	1.33	1.53	1.56
504032	50.00	4.00	32.00	477.32	29.40	6.46	6.99	9.50	9.58	2.02	2.16	17.60	16.80	0.89	1.13	0.77	1.09
505033	50.00	5.00	33.00	478.83	62.60	13.00	13.22	6.80	6.72	2.07	1.99	2.55	2.52	1.37	1.35	2.48	2.52
506012	50.00	6.00	12.00	480.12	30.70	6.88	7.37	10.60	10.58	2.14	2.16	14.60	13.86	0.87	1.02	1.08	1.20
511031	51.00	1.00	31.00	482.40	46.30	10.70	11.33	4.95	4.86	1.80	1.83	15.80	15.40	1.26	1.28	1.64	1.68
512036	51.00	2.00	36.00	483.96	38.00	8.85	9.45	4.17	4.15	1.58	1.58	21.30	19.60	1.06	1.13	1.15	1.32
513035	51.00	3.00	35.00	485.45	39.30	8.96	9.63	4.16	4.00	1.55	1.59	21.50	21.00	1.11	1.16	1.23	1.44
514068	51.00	4.00	68.00	487.28	4.84	1.10	1.25	16.40	17.16	2.47	2.66	18.90	18.20	0.33	0.65	0.07	0.17
515024	51.00	5.00	24.00	488.34	43.50	10.20	10.77	6.60	6.15	2.00	1.99	14.20	13.44	1.28	1.28	1.61	1.68
516083	51.00	6.00	83.00	490.43	—	3.40	—	18.59	—	3.15	—	12.60	—	0.65	—	0.48	
522010	52.00	2.00	10.00	493.40	31.30	7.09	7.56	8.38	7.86	1.99	1.99	19.70	18.20	0.92	1.06	0.92	1.10
523098	52.00	3.00	98.00	495.78	38.70	6.89	7.56	5.74	5.86	1.67	1.66	19.80	19.60	1.06	1.15	0.97	1.16
524056	52.00	4.00	56.00	496.86	38.20	8.34	9.07	3.85	3.86	1.40	1.48	23.50	22.40	1.03	1.12	1.18	1.44
525069	52.00	5.00	69.00	498.49	36.80	9.24	10.01	5.22	5.15	1.68	1.66	21.20	19.60	0.94	1.11	1.31	1.56
526076	52.00	6.00	76.00	500.06	59.20	14.00	14.36	9.81	9.87	2.45	2.32	1.34	1.36	1.24	1.32	3.23	3.24
531047	53.00	1.00	47.00	501.87	44.90	10.90	11.52	5.10	5.01	1.80	1.83	16.20	15.40	1.22	1.27	1.66	1.80
532008	53.00	2.00	8.00	502.98	60.00	14.10	14.36	8.79	9.01	2.27	2.32	0.77	0.80	1.33	1.29	2.72	2.76
533055	53.00	3.00	55.00	504.95	47.20	10.20	10.77	5.52	5.29	1.73	1.83	14.90	14.00	1.22	1.23	1.67	1.80
534079	53.00	4.00	79.00	506.45	—	2.27	—	17.16	—	2.66	—	15.40	—	0.81	—	0.32	
535018	53.00	5.00	18.00	507.58	42.30	9.90	10.39	5.41	5.15	1.67	1.66	18.50	18.20	1.10	1.15	1.55	1.68
541025	54.00	1.00	25.00	511.35	38.10	9.45	10.01	8.89	8.44	2.06	2.16	15.40	14.00	1.00	1.17	1.39	1.44
542013	54.00	2.00	13.00	512.73	40.30	9.04	9.82	5.43	5.43	1.69	1.83	19.00	18.20	1.09	1.19	1.29	1.44
543016	54.00	3.00	16.00	514.26	49.00	12.40	13.03	6.30	6.15	1.98	1.99	11.50	10.92	1.25	1.32	2.01	2.16
544123	54.00	4.00	123.00	516.83	60.40	13.00	13.41	9.63	9.72	2.18	2.16	2.60	2.66	1.14	1.19	2.72	2.88
545011	54.00	5.00	11.00	517.20	50.30	11.10	11.71	4.90	4.86	1.81	1.83	12.60	12.04	1.21	1.24	1.61	1.68
546014	54.00	6.00	14.00	518.74	40.40	8.19	8.69	3.61	3.72	1.33	1.39	22.40	21.00	1.03	1.06	1.08	1.20

**Table 1 (continued).**

Sample	Core	Section	Interval	Depth (m)	TiO <sub>2</sub> -xrf (%)	TiO <sub>2</sub> -icp (%)	P <sub>2</sub> O <sub>5</sub> -xrf (%)	P <sub>2</sub> O <sub>5</sub> -icp (%)	MnO-xrf (%)	MnO-icp (%)	LOI 900°C (%)	Ba (ppm)	Ce (ppm)	Co (ppm)	Cr (ppm)	Cu (ppm)	Ga (ppm)	La (ppm)
281089	28.00	1.00	89.00	260.99	0.47	0.40	0.10	0.09	0.08	0.08	19.50	830.00	58.00	20.00	72.00	56.00	14.00	26.00
282052	28.00	2.00	52.00	262.12	0.34	0.30	0.08	0.09	0.22	0.22	21.80	930.00	38.00	44.00	58.00	42.00	13.00	19.00
283054	28.00	3.00	54.00	263.65	0.31	0.28	0.09	0.09	0.13	0.14	26.90	640.00	44.00	16.00	51.00	47.00	11.00	19.00
284068	28.00	4.00	68.00	265.28	0.53	0.45	0.08	0.09	0.41	0.37	14.50	620.00	67.00	23.00	75.00	73.00	18.00	29.00
301051	30.00	1.00	51.00	279.93	0.31	0.27	0.11	0.11	4.60	4.39	27.00	450.00	46.00	15.00	46.00	45.00	30.00	21.00
302092	30.00	2.00	92.00	281.82	0.39	0.33	0.08	0.09	0.12	0.12	23.80	600.00	48.00	74.00	62.00	64.00	12.00	22.00
303045	30.00	3.00	45.00	282.85	0.33	0.32	0.11	0.11	0.17	0.18	27.00	520.00	44.00	23.00	53.00	54.00	11.00	21.00
304098	30.00	4.00	98.00	284.88	0.42	0.35	0.19	0.18	0.15	0.13	22.40	550.00	63.00	13.00	52.00	58.00	13.00	28.00
305112	30.00	5.00	112.00	286.52	0.47	0.40	0.16	0.16	0.14	0.13	20.60	530.00	55.00	81.00	60.00	60.00	13.00	25.00
306097	30.00	6.00	97.00	287.87	0.45	0.38	0.12	0.11	0.20	0.19	22.30	550.00	50.00	34.00	60.00	70.00	13.00	23.00
307029	30.00	7.00	29.00	288.69	0.54	0.43	0.09	0.09	0.07	0.08	18.10	740.00	64.00	74.00	79.00	74.00	16.00	26.00
311029	31.00	1.00	29.00	289.29	0.46	0.42	0.13	0.11	0.12	0.12	20.30	750.00	58.00	22.00	65.00	50.00	15.00	24.00
312102	31.00	2.00	102.00	291.51	0.42	0.38	0.13	0.11	1.55	1.29	21.30	640.00	55.00	25.00	50.00	70.00	21.00	23.00
321049	32.00	1.00	49.00	299.09	0.35	0.32	0.12	0.11	0.21	0.21	23.00	560.00	43.00	13.00	53.00	72.00	12.00	20.00
322032	32.00	2.00	32.00	300.42	0.34	0.30	0.13	0.14	0.14	0.14	19.10	610.00	47.00	20.00	51.00	60.00	10.00	20.00
332018	33.00	2.00	18.00	309.98	0.38	0.33	0.09	0.09	0.13	0.14	22.20	690.00	44.00	150.00	59.00	63.00	12.00	19.00
351028	35.00	1.00	28.00	327.88	0.49	0.38	0.08	0.07	0.08	0.08	17.70	650.00	55.00	33.00	65.00	54.00	14.00	25.00
352029	35.00	2.00	29.00	329.39	0.49	0.43	0.10	0.09	0.10	0.10	17.60	550.00	56.00	17.00	60.00	85.00	14.00	24.00
353024	35.00	3.00	24.00	332.63	0.47	0.40	0.09	0.09	0.07	0.08	17.80	650.00	53.00	19.00	59.00	60.00	14.00	24.00
361068	36.00	1.00	68.00	337.88	0.48	0.38	0.16	0.14	0.28	0.26	18.50	610.00	66.00	38.00	67.00	59.00	14.00	27.00
362068	36.00	2.00	68.00	339.38	0.46	0.42	0.08	0.09	0.17	0.07	16.90	820.00	62.00	30.00	74.00	70.00	15.00	27.00
363068	36.00	3.00	68.00	340.88	0.45	0.38	0.12	0.11	0.07	0.08	15.20	250.00	55.00	49.00	70.00	65.00	15.00	24.00
364041	36.00	4.00	42.00	342.13	—	0.12	—	0.21	—	11.48	—	190.00	54.00	19.00	20.00	12.00	—	24.00
364068	36.00	4.00	68.00	342.38	0.48	0.42	0.16	0.16	0.19	0.18	17.40	830.00	62.00	24.00	73.00	75.00	15.00	27.00
372014	37.00	2.00	15.00	348.35	0.45	0.38	0.09	0.09	0.07	0.08	18.60	610.00	50.00	31.00	67.00	80.00	14.00	22.00
373015	37.00	3.00	15.00	349.85	0.44	0.38	0.11	0.09	0.09	0.10	19.40	710.00	48.00	52.00	67.00	62.00	14.00	22.00
374015	37.00	4.00	15.00	351.35	0.38	0.33	0.06	0.07	0.10	0.10	20.50	510.00	44.00	16.00	59.00	56.00	12.00	19.00
381036	38.00	1.00	36.00	356.76	0.38	0.32	0.09	0.09	0.13	0.13	21.80	560.00	44.00	25.00	58.00	58.00	11.00	19.00
382040	38.00	2.00	39.00	358.30	0.41	0.35	0.08	0.07	0.07	0.08	18.40	590.00	51.00	19.00	66.00	70.00	12.00	22.00
383041	38.00	3.00	41.00	359.81	0.41	0.37	0.09	0.07	0.10	0.10	18.40	610.00	45.00	47.00	67.00	55.00	14.00	20.00
384041	38.00	4.00	41.00	361.31	0.36	0.32	0.09	0.09	0.15	0.15	21.50	620.00	41.00	43.00	58.00	53.00	12.00	18.00
385041	38.00	5.00	41.00	362.81	0.47	0.42	0.10	0.09	0.07	0.08	16.20	710.00	58.00	19.00	73.00	69.00	15.00	24.00
386066	38.00	6.00	67.00	364.56	—	0.08	—	1.56	—	12.90	—	160.00	51.00	35.00	16.00	11.00	—	31.00
391017	39.00	1.00	17.00	366.27	0.50	0.43	0.17	0.16	0.05	0.05	12.30	870.00	79.00	35.00	78.00	120.00	15.00	33.00
392017	39.00	2.00	17.00	367.77	0.44	0.38	0.13	0.11	0.11	0.11	15.90	770.00	59.00	22.00	68.00	73.00	14.00	25.00
393019	39.00	3.00	19.00	369.29	0.41	0.35	0.09	0.07	0.06	0.07	17.00	690.00	59.00	39.00	66.00	98.00	14.00	25.00
411030	41.00	1.00	30.00	385.70	0.35	0.30	0.12	0.11	3.34	3.35	21.50	630.00	55.00	14.00	51.00	49.00	19.00	24.00
412030	41.00	2.00	30.00	387.20	0.38	0.32	0.07	0.07	0.11	0.11	22.10	600.00	43.00	19.00	60.00	51.00	12.00	20.00
413030	41.00	3.00	30.00	388.70	0.39	0.32	0.11	0.11	0.13	0.13	22.20	560.00	53.00	15.00	58.00	79.00	12.00	23.00
414030	41.00	4.00	30.00	390.20	0.41	0.35	0.08	0.07	0.07	0.08	20.10	710.00	56.00	61.00	70.00	68.00	14.00	25.00
415030	41.00	5.00	30.00	391.70	0.28	0.25	0.17	0.16	5.60	5.55	24.50	540.00	58.00	71.00	39.00	57.00	—	24.00
416070	41.00	6.00	70.00	393.60	0.24	0.22	0.21	0.21	6.95	6.58	26.80	330.00	65.00	20.00	37.00	32.00	—	28.00
421042	42.00	1.00	42.00	395.52	0.42	0.37	0.07	0.07	0.09	0.10	21.80	650.00	50.00	19.00	66.00	69.00	15.00	23.00
422048	42.00	2.00	48.00	397.07	0.37	0.33	0.11	0.11	0.34	0.31	22.80	780.00	55.00	23.00	61.00	31.00	15.00	24.00
424014	42.00	4.00	14.00	399.74	0.36	0.32	0.14	0.14	0.40	0.37	23.20	730.00	59.00	12.00	45.00	33.00	15.00	26.00
425028	42.00	5.00	28.00	401.38	0.29	0.27	0.11	0.11	0.38	0.35	27.20	650.00	44.00	19.00	39.00	29.00	14.00	19.00
426047	42.00	6.00	47.00	403.07	0.36	0.32	0.09	0.09	0.39	0.37	25.40	570.00	41.00	19.00	61.00	240.00	14.00	20.00
427049	42.00	7.00	49.00	404.59	0.35	0.32	0.15	0.16	0.18	0.18	24.60	660.00	64.00	24.00	58.00	38.00	12.00	26.00
431086	43.00	1.00	86.00	405.66	0.37	0.32	0.13	0.11	0.25	0.25	22.10	710.00	53.00	32.00	50.00	180.00	13.00	24.00
432029	43.00	2.00	29.00	406.59	0.42	0.35	0.09	0.09	0.10	0.10	20.60	640.00	56.00	40.00	66.00	72.00	13.00	24.00
433083	43.00	3.00	83.00	408.63	0.46	0.38	0.43	0.41	0.69	0.61	16.90	820.00	110.00	130.00	70.00	41.00	19.00	42.00
434025	43.00	4.00	25.00	409.55	0.20	0.15	14.80	16.03	2.42	2.06	16.10	620.00	740.00	25.00	34.00	27.00	21.00	350.00
435018	43.00	5.00	18.00	410.98	0.36	0.32	0.19	0.18	2.01	1.93	22.60	660.00	73.00	90.00	56.00	58.00	—	29.00
436027	43.00	6.00	27.00	412.57	0.51	0.43	0.14	0.14	0.11	0.11	15.00	950.00	67.00	26.00	79.00	44.00	17.00	29.00
437026	43.00	7.00	26.00	414.06	0.51	0.43	0.13	0.11	0.08	0.09	16.50	760.00	70.00	35.00	82.00	66.00	17.00	29.00
441080	44.00	1.00	80.00	415.30	0.43	0.37	0.10	0.09	0.10	0.08	18.60	740.00	63.00	14.00	71.00	69.00	15.00	26.00
442082	44.00	2.00	82.00	416.82	0.46	0.38	0.10	0.09	0.19	0.19	18.00	730.00	66.00	33.00	58.00	98.00	16.00	28.00

443087	44.00	3.00	87.00	418.36	0.42	0.35	0.09	0.09	0.35	0.31	20.90	730.00	61.00	14.00	55.00	52.00	15.00	28.00
444116	44.00	4.00	116.00	420.16	0.36	0.33	0.09	0.09	0.33	0.31	23.80	680.00	49.00	14.00	59.00	37.00	14.00	23.00
445074	44.00	5.00	74.00	421.24	0.31	0.27	0.10	0.09	0.31	0.30	26.90	500.00	44.00	14.00	43.00	31.00	12.00	21.00
446064	44.00	6.00	64.00	422.64	0.38	0.33	0.06	0.07	0.23	0.22	24.00	550.00	52.00	23.00	54.00	41.00	14.00	24.00
451102	45.00	1.00	102.00	425.11	0.38	0.33	0.07	0.07	0.07	0.08	20.50	850.00	58.00	23.00	62.00	57.00	15.00	24.00
453055	45.00	3.00	55.00	427.65	0.35	0.30	0.07	0.07	0.08	0.09	21.10	790.00	52.00	100.00	63.00	77.00	14.00	23.00
461047	46.00	1.00	47.00	434.27	0.46	0.40	0.10	0.09	0.07	0.08	15.70	990.00	66.00	23.00	72.00	79.00	14.00	28.00
462041	46.00	2.00	41.00	435.71	0.39	0.35	0.08	0.07	0.08	0.09	18.80	1100.00	70.00	9.00	67.00	74.00	13.00	28.00
463041	46.00	3.00	41.00	437.21	0.45	0.38	0.10	0.09	0.07	0.07	16.30	1100.00	68.00	310.00	74.00	81.00	13.00	28.00
464041	46.00	4.00	41.00	438.71	0.57	0.50	0.08	0.07	0.05	0.06	13.30	720.00	70.00	18.00	83.00	85.00	15.00	29.00
465057	46.00	5.00	57.00	440.37	0.52	0.43	0.10	0.09	0.09	0.09	14.90	700.00	70.00	27.00	77.00	88.00	15.00	29.00
465111	46.00	5.00	111.00	440.91	0.31	0.22	11.30	12.37	0.23	0.22	14.50	730.00	860.00	15.00	48.00	69.00	11.00	410.00
466057	46.00	6.00	57.00	441.87	0.50	0.43	0.09	0.09	0.08	0.08	16.20	650.00	72.00	23.00	74.00	86.00	15.00	29.00
471033	47.00	1.00	33.00	443.82	0.47	0.42	0.08	0.07	0.09	0.10	15.80	810.00	45.00	14.00	80.00	36.00	14.00	20.00
473016	47.00	3.00	16.00	446.66	0.50	0.42	0.10	0.09	0.07	0.07	14.80	840.00	73.00	45.00	76.00	74.00	15.00	30.00
474021	47.00	4.00	21.00	448.21	0.46	0.40	0.07	0.07	0.30	0.28	16.70	770.00	66.00	33.00	70.00	78.00	16.00	28.00
475021	47.00	5.00	21.00	449.71	0.35	0.30	0.07	0.07	0.07	0.08	20.80	780.00	46.00	14.00	59.00	52.00	12.00	21.00
476025	47.00	6.00	25.00	451.25	0.51	0.40	0.08	0.07	0.03	0.04	8.38	820.00	130.00	34.00	96.00	130.00	15.00	55.00
481007	48.00	1.00	7.00	453.27	—	0.10	—	0.09	—	11.48	—	260.00	36.00	32.00	21.00	18.00	—	17.00
481030	48.00	1.00	30.00	453.50	0.44	0.38	0.07	0.07	0.24	0.23	13.20	1000.00	66.00	18.00	68.00	57.00	15.00	30.00
482034	48.00	2.00	34.00	455.04	0.38	0.33	0.08	0.09	0.07	0.08	20.20	590.00	58.00	22.00	59.00	75.00	12.00	25.00
483029	48.00	3.00	29.00	456.49	0.44	0.37	0.07	0.07	0.04	0.05	13.20	890.00	68.00	59.00	71.00	39.00	14.00	29.00
484032	48.00	4.00	32.00	458.02	0.46	0.40	0.13	0.11	0.12	0.12	15.40	830.00	78.00	51.00	70.00	73.00	16.00	30.00
485030	48.00	5.00	30.00	459.50	0.51	0.43	0.07	0.07	0.04	0.05	10.70	580.00	93.00	140.00	76.00	63.00	16.00	37.00
491074	49.00	1.00	74.00	463.54	0.44	0.38	0.12	0.11	0.58	0.52	16.20	870.00	57.00	32.00	70.00	64.00	18.00	24.00
492066	49.00	2.00	66.00	464.96	0.44	0.38	0.08	0.09	0.09	0.09	16.10	630.00	62.00	50.00	69.00	78.00	15.00	26.00
493080	49.00	3.00	80.00	466.60	0.31	0.27	0.12	0.11	5.81	5.55	22.90	570.00	76.00	26.00	44.00	53.00	31.00	31.00
494039	49.00	4.00	39.00	467.69	0.32	0.28	0.11	0.09	2.61	2.58	21.70	780.00	69.00	100.00	47.00	55.00	27.00	28.00
496043	49.00	6.00	43.00	470.73	0.27	0.25	0.07	0.07	0.17	0.17	21.10	630.00	36.00	25.00	48.00	58.00	10.00	16.00
501056	50.00	1.00	56.00	473.06	0.37	0.32	0.15	0.14	0.82	0.72	18.20	810.00	67.00	15.00	51.00	61.00	15.00	27.00
502056	50.00	2.00	56.00	474.56	0.40	0.33	0.06	0.07	0.10	0.10	18.00	610.00	52.00	45.00	62.00	84.00	12.00	23.00
503036	50.00	3.00	36.00	475.86	0.41	0.35	0.07	0.07	0.09	0.09	17.00	830.00	58.00	23.00	66.00	110.00	13.00	25.00
504032	50.00	4.00	32.00	477.32	0.23	0.20	2.01	2.04	7.86	7.74	23.30	2100.00	160.00	31.00	41.00	50.00	—	62.00
505033	50.00	5.00	33.00	478.83	0.47	0.38	0.08	0.07	0.06	0.06	8.41	640.00	87.00	36.00	90.00	68.00	16.00	37.00
506012	50.00	6.00	12.00	480.12	0.24	0.22	0.15	0.14	9.58	9.42	23.30	720.00	97.00	16.00	39.00	57.00	—	38.00
511031	51.00	1.00	31.00	482.40	0.40	0.35	0.07	0.07	0.23	0.22	17.00	1000.00	58.00	19.00	66.00	110.00	14.00	26.00
512036	51.00	2.00	36.00	483.96	0.30	0.27	0.10	0.09	0.80	0.70	22.30	840.00	53.00	23.00	52.00	65.00	16.00	23.00
513035	51.00	3.00	35.00	485.45	0.32	0.28	0.06	0.07	0.21	0.21	19.60	670.00	57.00	47.00	55.00	62.00	11.00	25.00
514068	51.00	4.00	68.00	487.28	0.04	0.05	7.31	8.24	20.20	19.35	27.70	3200.00	620.00	16.00	17.00	8.00	—	220.00
515024	51.00	5.00	24.00	488.34	0.37	0.33	0.12	0.11	2.37	2.45	18.20	940.00	53.00	21.00	60.00	50.00	18.00	23.00
516083	51.00	6.00	83.00	490.43	—	0.08	—	0.55	—	15.48	—	490.00	120.00	39.00	20.00	14.00	—	45.00
522010	52.00	2.00	10.00	493.40	0.24	0.22	0.78	0.80	5.48	5.29	24.00	610.00	110.00	14.00	44.00	160.00	14.00	44.00
523098	52.00	3.00	98.00	495.78	0.22	0.20	0.11	0.11	3.28	3.22	22.30	780.00	45.00	11.00	44.00	59.00	—	19.00
524056	52.00	4.00	56.00	496.86	0.30	0.27	0.08	0.09	0.13	0.13	22.40	700.00	59.00	70.00	55.00	71.00	12.00	24.00
525069	52.00	5.00	69.00	498.49	0.34	0.30	0.10	0.09	1.67	1.68	21.70	730.00	55.00	23.00	41.00	69.00	—	24.00
526076	52.00	6.00	76.00	500.06	0.48	0.42	0.06	0.07	0.03	0.04	8.10	720.00	110.00	18.00	97.00	71.00	17.00	44.00
531047	53.00	1.00	47.00	501.87	0.42	0.37	0.11	0.09	0.15	0.15	17.30	620.00	78.00	17.00	54.00	97.00	15.00	32.00
532008	53.00	2.00	8.00	502.98	0.50	0.43	0.06	0.07	0.02L	0.03	8.81	650.00	86.00	86.00	94.00	50.00	17.00	38.00
533055	53.00	3.00	55.00	504.95	0.38	0.32	0.07	0.07	0.13	0.13	16.60	580.00	48.00	190.00	60.00	70.00	13.00	22.00
534079	53.00	4.00	79.00	506.45	—	0.05	—	7.56	—	16.77	—	1700.00	600.00	61.00	18.00	21.00	—	180.00
535018	53.00	5.00	18.00	507.58	0.39	0.33	0.09	0.09	0.18	0.17	18.60	590.00	59.00	62.00	52.00	75.00	12.00	26.00
541025	54.00	1.00	25.00	511.35	0.39	0.33	0.19	0.18	3.24	3.22	19.70	690.00	70.00	19.00	57.00	51.00	19.00	28.00
542013	54.00	2.00	13.00	512.73	0.35	0.32	0.09	0.09	1.36	1.12	20.10	680.00	44.00	27.00	59.00	80.00	19.00	19.00
543016	54.00	3.00	16.00	514.26	0.54	0.47	0.09	0.09	0.08	0.08	14.00	670.00	77.00	35.00	80.00	78.00	17.00	32.00
544123	54.00	4.00	123.00	516.83	0.45	0.40	0.06	0.05	0.03	0.04	7.80	760.00	110.00	21.00	83.00	61.00	18.00	43.00
545011	54.00	5.00	11.00	517.20	0.48	0.42	0.11	0.09	0.54	0.49	14.60	640.00	70.00	21.00	73.00	64.00	17.00	29.00
546014	54.00	6.00	14.00	518.74	0.30	0.28	0.11	0.09	0.20	0.19	21.10	610.00	50.00	19.00	48.00	46.00	11.00	21.00

Table 1 (continued).

Sample	Core	Section	Interval	Depth (m)	Li (ppm)	Nb (ppm)	Nd (ppm)	Ni (ppm)	Pb (ppm)	Sc (ppm)	Sr (ppm)	Th (ppm)	V (ppm)	Y (ppm)	Yb (ppm)	Zn (ppm)	CaCO <sub>3</sub> -ca (%)	CaCO <sub>3</sub> -cc (%)
281089	28.00	1.00	89.00	260.99	30.00	6.00	23.00	51.00	14.00	10.00	780.00	9.00	150.00	14.00	1.00	86.00	33.21	30.83
282052	28.00	2.00	52.00	262.12	25.00	4.00	16.00	110.00	19.00	9.00	840.00	7.00	110.00	11.00	1.00	58.00	37.86	35.92
283054	28.00	3.00	54.00	263.65	24.00	5.00	16.00	43.00	11.00	8.00	1100.00	5.00	110.00	12.00	1.00	74.00	51.61	48.25
284068	28.00	4.00	68.00	265.28	34.00	5.00	23.00	84.00	16.00	12.00	520.00	9.00	130.00	14.00	2.00	140.00	21.25	20.00
301051	30.00	1.00	51.00	279.93	23.00	4.00	17.00	42.00	10.00	9.00	800.00	15.00	86.00	15.00	2.00	89.00	41.79	50.92
302092	30.00	2.00	92.00	281.82	28.00	4.00	19.00	58.00	14.00	9.00	940.00	7.00	110.00	12.00	1.00	140.00	43.93	40.92
303045	30.00	3.00	45.00	282.85	25.00	<4.00	16.00	39.00	13.00	8.00	1000.00	6.00	99.00	15.00	1.00	67.00	52.14	49.67
304098	30.00	4.00	98.00	284.88	28.00	<4.00	22.00	41.00	15.00	10.00	840.00	7.00	120.00	20.00	2.00	82.00	41.25	38.67
305112	30.00	5.00	112.00	286.52	30.00	5.00	20.00	53.00	17.00	10.00	780.00	7.00	110.00	17.00	2.00	92.00	37.14	34.42
306097	30.00	6.00	97.00	287.87	27.00	6.00	20.00	48.00	16.00	10.00	800.00	7.00	110.00	15.00	2.00	86.00	40.18	37.58
307029	30.00	7.00	29.00	288.69	34.00	6.00	22.00	77.00	16.00	12.00	620.00	9.00	140.00	12.00	1.00	92.00	29.46	27.17
311029	31.00	1.00	29.00	289.29	27.00	5.00	20.00	64.00	14.00	11.00	780.00	8.00	120.00	15.00	2.00	85.00	36.25	33.58
312102	31.00	2.00	102.00	291.51	26.00	6.00	19.00	55.00	12.00	10.00	800.00	7.00	110.00	14.00	2.00	93.00	35.71	37.17
321049	32.00	1.00	49.00	299.09	21.00	5.00	15.00	36.00	11.00	8.00	1000.00	6.00	110.00	12.00	1.00	63.00	45.00	42.42
322032	32.00	2.00	32.00	300.42	20.00	<4.00	16.00	61.00	14.00	8.00	860.00	5.00	100.00	12.00	1.00	61.00	37.32	34.08
332018	33.00	2.00	18.00	309.98	23.00	5.00	17.00	39.00	12.00	9.00	970.00	44.00	120.00	10.00	1.00	67.00	41.79	36.67
351028	35.00	1.00	28.00	327.88	32.00	<4.00	22.00	53.00	12.00	11.00	550.00	34.00	130.00	13.00	1.00	87.00	28.93	26.58
352029	35.00	2.00	29.00	329.39	31.00	7.00	22.00	52.00	14.00	11.00	590.00	7.00	140.00	15.00	2.00	100.00	30.54	28.33
353024	35.00	3.00	24.00	332.63	32.00	<4.00	22.00	55.00	16.00	11.00	610.00	9.00	140.00	13.00	2.00	110.00	30.36	28.17
361068	36.00	1.00	68.00	337.88	31.00	<4.00	26.00	78.00	16.00	11.00	590.00	6.00	120.00	18.00	2.00	91.00	30.54	26.33
362068	36.00	2.00	68.00	339.38	32.00	6.00	23.00	84.00	13.00	12.00	590.00	8.00	130.00	13.00	2.00	97.00	27.50	25.58
363068	36.00	3.00	68.00	340.88	31.00	6.00	21.00	140.00	18.00	11.00	600.00	9.00	130.00	15.00	2.00	99.00	26.79	21.67
364041	36.00	4.00	42.00	342.13	13.00	<4.00	18.00	16.00	5.00	7.00	220.00	<4.00	45.00	18.00	2.00	33.00	16.50	71.00
364068	36.00	4.00	68.00	342.38	29.00	5.00	25.00	72.00	19.00	11.00	690.00	9.00	130.00	16.00	2.00	100.00	28.75	26.92
372014	37.00	2.00	15.00	348.35	31.00	6.00	20.00	89.00	19.00	10.00	740.00	8.00	140.00	12.00	1.00	110.00	31.96	23.17
373015	37.00	3.00	15.00	349.85	32.00	6.00	20.00	45.00	17.00	10.00	810.00	8.00	130.00	12.00	1.00	83.00	35.18	32.00
374015	37.00	4.00	15.00	351.35	29.00	<4.00	16.00	37.00	11.00	9.00	810.00	6.00	120.00	10.00	1.00	87.00	37.32	35.17
381036	38.00	1.00	36.00	356.76	26.00	<4.00	17.00	46.00	12.00	9.00	860.00	6.00	100.00	11.00	1.00	69.00	41.25	38.33
382040	38.00	2.00	39.00	358.30	29.00	4.00	20.00	39.00	13.00	10.00	710.00	7.00	120.00	11.00	1.00	83.00	32.32	30.25
383041	38.00	3.00	41.00	359.81	29.00	5.00	16.00	49.00	14.00	10.00	710.00	9.00	130.00	11.00	1.00	72.00	31.96	29.58
384041	38.00	4.00	41.00	361.31	27.00	5.00	13.00	52.00	12.00	9.00	850.00	7.00	110.00	10.00	1.00	68.00	38.75	37.33
385041	38.00	5.00	41.00	362.81	32.00	6.00	22.00	50.00	15.00	11.00	610.00	9.00	140.00	12.00	2.00	91.00	26.61	24.42
386066	38.00	6.00	67.00	364.56	11.00	<4.00	13.00	27.00	4.00	5.00	200.00	<4.00	25.00	27.00	2.00	29.00	17.00	70.75
391017	39.00	1.00	17.00	366.27	38.00	8.00	34.00	120.00	27.00	12.00	450.00	8.00	160.00	21.00	2.00	100.00	17.09	15.50
392017	39.00	2.00	17.00	367.77	32.00	6.00	23.00	74.00	18.00	11.00	670.00	7.00	130.00	14.00	2.00	77.00	28.04	26.08
393019	39.00	3.00	19.00	369.29	32.00	6.00	22.00	56.00	16.00	11.00	690.00	8.00	130.00	13.00	2.00	82.00	28.75	26.75
411030	41.00	1.00	30.00	385.70	26.00	4.00	24.00	45.00	17.00	10.00	600.00	5.00	110.00	17.00	2.00	64.00	29.29	40.17
412030	41.00	2.00	30.00	387.20	25.00	<4.00	16.00	41.00	13.00	10.00	880.00	14.00	110.00	10.00	1.00	75.00	42.14	38.83
413030	41.00	3.00	30.00	388.70	25.00	<4.00	20.00	53.00	18.00	9.00	910.00	6.00	110.00	15.00	2.00	83.00	42.86	40.17
414030	41.00	4.00	30.00	390.20	28.00	5.00	20.00	54.00	14.00	11.00	860.00	9.00	140.00	11.00	1.00	76.00	35.71	33.08
415030	41.00	5.00	30.00	391.70	21.00	<4.00	20.00	110.00	14.00	9.00	640.00	4.00	88.00	18.00	2.00	77.00	30.89	47.92
416070	41.00	6.00	70.00	393.60	21.00	<4.00	22.00	44.00	9.00	9.00	600.00	5.00	87.00	21.00	2.00	82.00	30.71	54.58
421042	42.00	1.00	42.00	395.52	29.00	5.00	17.00	46.00	18.00	11.00	850.00	8.00	140.00	11.00	1.00	85.00	39.29	36.83
422048	42.00	2.00	48.00	397.07	26.00	5.00	22.00	44.00	15.00	10.00	950.00	8.00	120.00	15.00	2.00	83.00	41.79	40.25
424014	42.00	4.00	14.00	399.74	26.00	5.00	22.00	42.00	16.00	10.00	980.00	8.00	110.00	16.00	2.00	72.00	43.21	41.92
425028	42.00	5.00	28.00	401.38	23.00	4.00	17.00	37.00	13.00	8.00	1200.00	8.00	100.00	12.00	1.00	59.00	52.32	50.50
426047	42.00	6.00	47.00	403.07	27.00	5.00	16.00	46.00	15.00	9.00	1100.00	8.00	120.00	11.00	1.00	93.00	48.75	47.00
427049	42.00	7.00	49.00	404.59	25.00	<4.00	26.00	39.00	10.00	10.00	970.00	6.00	97.00	19.00	2.00	62.00	47.14	43.83
431086	43.00	1.00	86.00	405.66	26.00	<4.00	22.00	76.00	21.00	10.00	840.00	7.00	120.00	16.00	2.00	100.00	40.54	37.83
432029	43.00	2.00	29.00	406.59	29.00	<4.00	22.00	70.00	16.00	11.00	810.00	7.00	120.00	13.00	2.00	100.00	37.50	34.25
433083	43.00	3.00	83.00	408.63	30.00	5.00	41.00	88.00	18.00	12.00	580.00	9.00	130.00	36.00	3.00	83.00	25.89	24.00
434025	43.00	4.00	25.00	409.55	16.00	5.00	260.00	36.00	9.00	14.00	1100.00	<4.00	71.00	480.00	28.00	48.00	55.89	24.17
435018	43.00	5.00	18.00	410.98	26.00	5.00	27.00	60.00	12.00	11.00	820.00	6.00	98.00	22.00	2.00	95.00	39.46	41.50
436027	43.00	6.00	27.00	412.57	31.00	7.00	28.00	84.00	20.00	13.00	540.00	9.00	140.00	18.00	2.00	70.00	21.61	20.00
437026	43.00	7.00	26.00	414.06	33.00	7.00	29.00	65.00	22.00	13.00	600.00	9.00	190.00	18.00	2.00	110.00	23.75	21.42
441080	44.00	1.00	80.00	415.30	30.00	6.00	23.00	55.00	15.00	12.00	760.00	8.00	140.00	15.00	2.00	90.00	33.39	31.25
442082	44.00	2.00	82.00	416.82	31.00	9.00	26.00	80.00	20.00	12.00	680.00	8.00	130.00	16.00	2.00</			

443087	44.00	3.00	87.00	418.36	29.00	5.00	22.00	43.00	18.00	11.00	740.00	8.00	99.00	14.00	2.00	73.00	38.93	36.50
444116	44.00	4.00	116.00	420.16	28.00	7.00	18.00	43.00	11.00	10.00	890.00	8.00	89.00	13.00	1.00	52.00	45.71	43.92
445074	44.00	5.00	74.00	421.24	24.00	<4.00	17.00	31.00	10.00	8.00	950.00	7.00	83.00	13.00	1.00	52.00	53.39	50.17
446064	44.00	6.00	64.00	422.64	25.00	5.00	17.00	43.00	12.00	9.00	890.00	7.00	85.00	10.00	1.00	54.00	45.36	43.00
451102	45.00	1.00	102.00	425.11	28.00	5.00	21.00	54.00	13.00	11.00	760.00	8.00	110.00	14.00	2.00	91.00	36.61	34.75
453055	45.00	3.00	55.00	427.65	27.00	4.00	19.00	54.00	14.00	11.00	800.00	7.00	110.00	13.00	1.00	88.00	39.82	34.08
461047	46.00	1.00	47.00	434.27	31.00	6.00	27.00	68.00	17.00	12.00	530.00	9.00	150.00	19.00	2.00	75.00	25.00	22.75
462041	46.00	2.00	41.00	435.71	29.00	5.00	25.00	43.00	18.00	11.00	760.00	8.00	170.00	16.00	2.00	44.00	34.11	32.08
463041	46.00	3.00	41.00	437.21	30.00	<4.00	29.00	77.00	19.00	12.00	510.00	11.00	140.00	18.00	2.00	65.00	24.64	21.67
464041	46.00	4.00	41.00	438.71	35.00	7.00	29.00	49.00	19.00	14.00	390.00	9.00	220.00	16.00	2.00	100.00	17.75	16.17
465057	46.00	5.00	57.00	440.37	31.00	7.00	27.00	78.00	22.00	12.00	490.00	9.00	160.00	14.00	2.00	80.00	23.75	21.92
465111	46.00	5.00	111.00	440.91	20.00	5.00	280.00	47.00	14.00	14.00	910.00	<4.00	110.00	430.00	24.00	62.00	50.18	21.92
466057	46.00	6.00	57.00	441.87	31.00	9.00	27.00	71.00	16.00	12.00	520.00	10.00	160.00	16.00	2.00	100.00	25.36	23.33
471033	47.00	1.00	33.00	443.82	32.00	7.00	18.00	55.00	18.00	12.00	490.00	9.00	160.00	11.00	1.00	50.00	23.39	22.00
473016	47.00	3.00	16.00	446.66	33.00	6.00	28.00	46.00	16.00	13.00	450.00	10.00	160.00	18.00	2.00	88.00	21.79	19.83
474021	47.00	4.00	21.00	448.21	32.00	7.00	26.00	53.00	12.00	14.00	550.00	11.00	160.00	17.00	2.00	110.00	24.46	25.00
475021	47.00	5.00	21.00	449.71	27.00	6.00	18.00	40.00	14.00	10.00	780.00	9.00	120.00	15.00	2.00	56.00	37.86	35.75
476025	47.00	6.00	25.00	451.25	37.00	8.00	54.00	86.00	27.00	12.00	150.00	17.00	290.00	27.00	3.00	100.00	1.73	0.75
481007	48.00	1.00	7.00	453.27	14.00	<4.00	13.00	26.00	6.00	4.00	120.00	<4.00	41.00	17.00	2.00	69.00	11.00	69.75
481030	48.00	1.00	30.00	453.50	41.00	6.00	26.00	59.00	18.00	13.00	410.00	11.00	170.00	13.00	2.00	73.00	16.50	15.67
482034	48.00	2.00	34.00	455.04	31.00	<4.00	24.00	48.00	11.00	11.00	730.00	6.00	140.00	17.00	2.00	110.00	36.43	34.00
483029	48.00	3.00	29.00	456.49	36.00	6.00	26.00	90.00	19.00	13.00	440.00	8.00	130.00	15.00	2.00	69.00	18.93	16.75
484032	48.00	4.00	32.00	458.02	35.00	6.00	28.00	78.00	20.00	13.00	530.00	9.00	130.00	19.00	2.00	99.00	24.46	22.08
485030	48.00	5.00	30.00	459.50	37.00	6.00	34.00	81.00	20.00	14.00	310.00	11.00	140.00	15.00	2.00	110.00	11.32	9.83
491074	49.00	1.00	74.00	463.54	32.00	6.00	24.00	54.00	17.00	13.00	560.00	11.00	140.00	17.00	2.00	92.00	25.36	23.75
492066	49.00	2.00	66.00	464.96	31.00	6.00	24.00	67.00	17.00	12.00	590.00	9.00	160.00	15.00	2.00	100.00	24.64	22.57
493080	49.00	3.00	80.00	466.60	24.00	5.00	27.00	38.00	10.00	10.00	600.00	18.00	100.00	21.00	3.00	62.00	30.89	41.83
494039	49.00	4.00	39.00	467.69	25.00	5.00	26.00	79.00	21.00	10.00	670.00	13.00	120.00	18.00	2.00	61.00	33.57	35.00
496043	49.00	6.00	43.00	470.73	28.00	<4.00	12.00	49.00	11.00	9.00	790.00	6.00	110.00	10.00	1.00	83.00	43.36	38.33
501056	50.00	1.00	56.00	473.06	28.00	5.00	30.00	43.00	14.00	11.00	620.00	7.00	120.00	20.00	2.00	81.00	30.54	29.67
502056	50.00	2.00	56.00	474.56	29.00	5.00	21.00	71.00	20.00	12.00	580.00	9.00	140.00	12.00	2.00	92.00	27.86	25.25
503036	50.00	3.00	36.00	475.86	30.00	4.00	23.00	56.00	18.00	12.00	580.00	9.00	170.00	12.00	1.00	120.00	27.86	24.75
504032	50.00	4.00	32.00	477.32	21.00	4.00	67.00	47.00	10.00	9.00	640.00	<4.00	95.00	82.00	5.00	73.00	31.43	43.83
505033	50.00	5.00	33.00	478.83	38.00	6.00	32.00	59.00	20.00	12.00	190.00	14.00	190.00	11.00	1.00	80.00	4.55	3.42
506012	50.00	6.00	12.00	480.12	22.00	<4.00	34.00	48.00	12.00	9.00	500.00	4.00	100.00	30.00	4.00	85.00	26.07	43.92
511031	51.00	1.00	31.00	482.40	29.00	5.00	23.00	58.00	16.00	11.00	630.00	10.00	160.00	13.00	2.00	120.00	28.21	25.33
512036	51.00	2.00	36.00	483.96	24.00	4.00	24.00	52.00	14.00	10.00	820.00	8.00	120.00	16.00	2.00	87.00	38.04	36.08
513035	51.00	3.00	35.00	485.45	25.00	6.00	23.00	61.00	13.00	10.00	780.00	8.00	110.00	13.00	2.00	76.00	38.39	34.58
514068	51.00	4.00	68.00	487.28	9.00	<4.00	300.00	15.00	<4.00	7.00	760.00	43.00	28.00	300.00	16.00	85.00	33.75	63.92
515024	51.00	5.00	24.00	488.34	27.00	5.00	24.00	59.00	16.00	11.00	520.00	8.00	120.00	20.00	2.00	54.00	25.36	28.00
516083	51.00	6.00	83.00	490.43	15.00	<4.00	57.00	39.00	8.00	7.00	350.00	<4.00	59.00	54.00	5.00	38.00	22.50	65.67
522010	52.00	2.00	10.00	493.40	23.00	<4.00	48.00	29.00	19.00	9.00	730.00	<4.00	150.00	49.00	3.00	300.00	35.18	45.83
523098	52.00	3.00	98.00	495.78	29.00	<4.00	17.00	23.00	8.00	7.00	730.00	5.00	93.00	18.00	2.00	33.00	35.36	41.17
524056	52.00	4.00	56.00	496.86	26.00	<4.00	21.00	35.00	10.00	9.00	910.00	7.00	110.00	16.00	2.00	51.00	41.96	39.08
525069	52.00	5.00	69.00	498.49	24.00	4.00	22.00	51.00	14.00	10.00	790.00	8.00	130.00	20.00	2.00	75.00	37.86	39.25
526076	52.00	6.00	76.00	500.06	34.00	8.00	41.00	58.00	18.00	13.00	170.00	17.00	260.00	14.00	2.00	83.00	2.39	1.50
531047	53.00	1.00	47.00	501.87	28.00	5.00	30.00	60.00	28.00	12.00	670.00	10.00	160.00	18.00	2.00	110.00	28.93	26.08
532008	53.00	2.00	8.00	502.98	36.00	10.00	33.00	51.00	10.00	13.00	150.00	17.00	230.00	12.00	2.00	65.00	1.38	0.42
533055	53.00	3.00	55.00	504.95	30.00	5.00	19.00	260.00	24.00	11.00	580.00	8.00	150.00	12.00	1.00	68.00	26.61	24.25
534079	53.00	4.00	79.00	506.45	10.00	<4.00	340.00	18.00	<4.00	8.00	590.00	<4.00	60.00	330.00	20.00	380.00	27.50	58.92
535018	53.00	5.00	18.00	507.58	27.00	<4.00	26.00	62.00	14.00	11.00	680.00	7.00	130.00	16.00	2.00	82.00	33.04	30.42
541025	54.00	1.00	25.00	511.35	24.00	4.00	29.00	54.00	16.00	11.00	570.00	7.00	130.00	20.00	2.00	67.00	27.50	35.58
542013	54.00	2.00	13.00	512.73	27.00	5.00	15.00	70.00	14.00	10.00	730.00	7.00	120.00	13.00	2.00	68.00	33.93	30.75
543016	54.00	3.00	16.00	514.26	30.00	7.00	28.00	73.00	15.00	14.00	490.00	12.00	170.00	16.00	2.00	89.00	20.54	18.33
544123	54.00	4.00	123.00	516.83	38.00	7.00	38.00	75.00	20.00	13.00	190.00	19.00	190.00	12.00	2.00	70.00	4.64	3.67
545011	54.00	5.00	11.00	517.20	31.00	6.00	27.00	64.00	17.00	12.00	550.00	9.00	150.00	17.00	2.00	90.00	22.50	20.75
546014	54.00	6.00	14.00	518.74	25.00	4.00	19.00	41.00	14.00	9.00	840.00	7.00	110.00	14.00	1.00	68.00	40.00	37.92

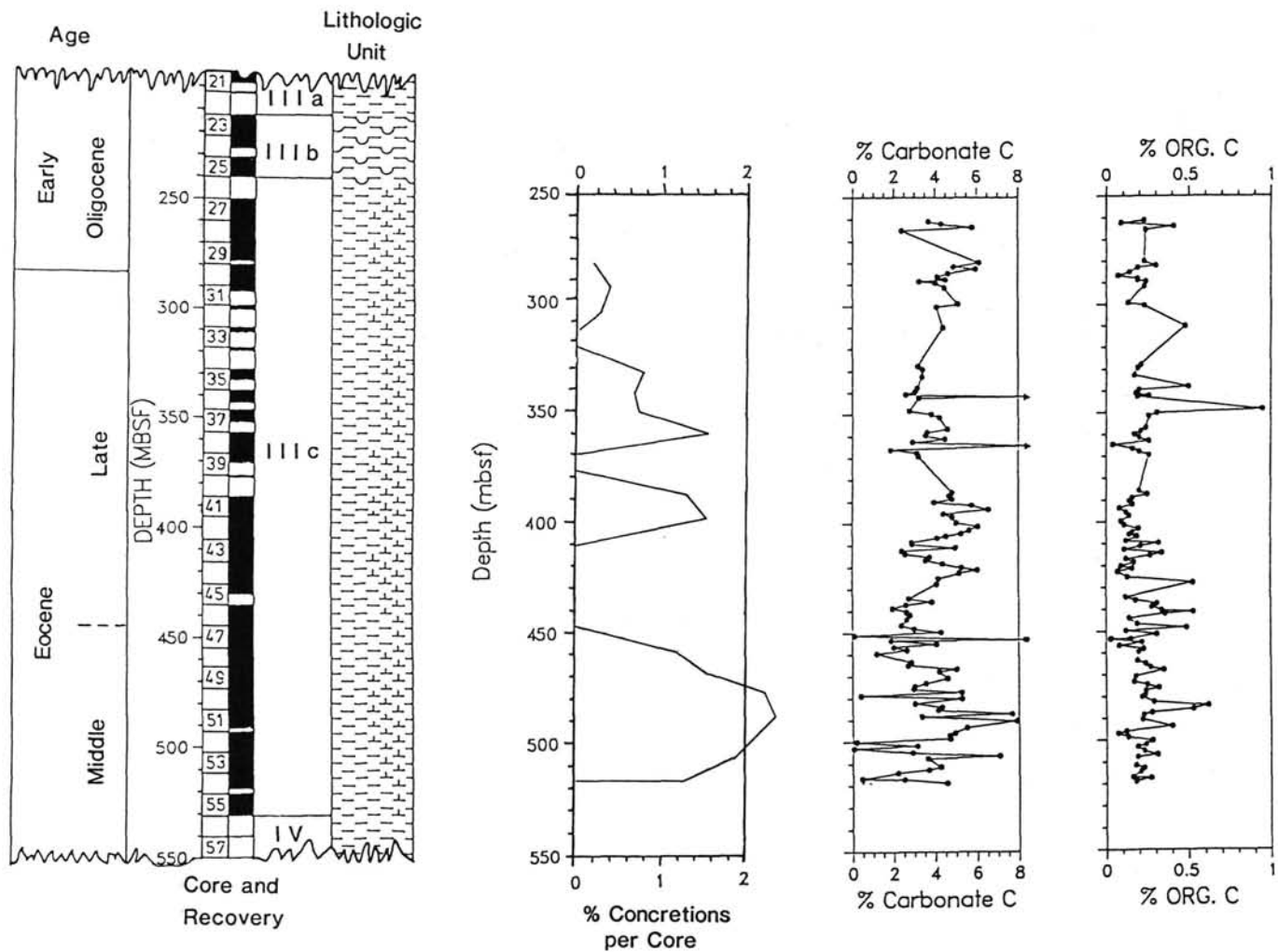


Figure 1. Age and lithology with depth for part of ODP Site 647 analyzed here. Percentage of concretionary layers per core (see Table 4), percent of carbonate carbon, and percent of organic carbon data from this study also are shown.

## RESULTS

### Carbon and Carbonate Data

Concentrations of organic carbon (OC) and carbonate carbon (CC) are shown plotted vs. depth, core recovery, age, and lithologic units in Figure 1. The scale is the same as that of the geochemical plots that follow (Figs. 2 through 7). The samples cover the middle Eocene through lower Oligocene interval, encompassing lithologic Unit IIIC but not including the biogenic silica-rich interval that constitutes lithologic Unit IIIB.

The OC content of most samples is low, below 0.5 wt%, and the average for lithologic Unit IIIB is about 0.25 wt%. The CC is highly variable (multiply CC by 8.33 to obtain approximate  $\text{CaCO}_3$  content; see first column, Fig. 2, and last column, Table 1), and highest values correspond to intervals in which carbonate nodules or concretionary layers occur. The relative abundance of such intervals also is plotted in Figure 1.

### Inorganic Geochemistry

The concentrations of major-element oxides plotted in Figure 2 are from XRF analyses, except for the five samples having high concentrations of Fe and Mn, for which no XRF analyses exist (Table 1). There are no  $\text{SiO}_2$  results for these five samples, but the  $\text{SiO}_2$  concentrations are estimated at 10% to 12%, based on the  $\text{Al}_2\text{O}_3$  concentrations and the  $\text{SiO}_2/\text{Al}_2\text{O}_3$  ratios of adja-

cent samples. Trace elements are grouped in Figures 3 through 6, according to similarities of patterns of the downhole plots. The concentration plots for chromium (Cr), lithium (Li), vanadium (V), scandium (Sc), and lead (Pb) (Fig. 3) all have similar patterns that are also similar to those of the major elements representative of a detrital fraction (e.g.,  $\text{Al}_2\text{O}_3$  and  $\text{TiO}_2$ , Fig. 2), indicating that these trace elements are primarily associated with the clastic (clay) fraction. The concentration plots of the rare-earth elements (REE) cerium (Ce), lanthanum (La), neodymium (Nd), yttrium (Y), and ytterbium (Yb) (Fig. 4) are similar to one another and resemble the downhole plot of  $\text{P}_2\text{O}_5$  (Fig. 2), suggesting that the REEs mainly are associated with one or more phosphate minerals, at least where the peaks of higher concentration are concerned.

The downhole plot of strontium (Sr) concentration (Fig. 5) parallels that of  $\text{CaO}$  (Fig. 2), indicating that Sr probably was substituted for Ca in one or more Ca-bearing mineral phases. However, the Sr and  $\text{CaO}$  concentrations do not always correlate with those in the downhole plot of  $\text{CaCO}_3$  (Fig. 1). The concentration of  $\text{CaCO}_3$  was calculated by assuming that all of the CC was derived from  $\text{CaCO}_3$  ( $\text{CaCO}_3 = \text{CC} \times 8.33$ ). However, as we discuss later, this assumption is not always true for the present set of samples. In most other data sets of carbonate-rich, deep-sea sediments and rocks that we have analyzed (e.g., Dean and Parduhn, 1984; Arthur et al., 1987), the concentra-

GEOCHEMICAL EXPRESSION OF EARLY DIAGENESIS IN  
MIDDLE EOCENE-LOWER OLIGOCENE SEDIMENTS

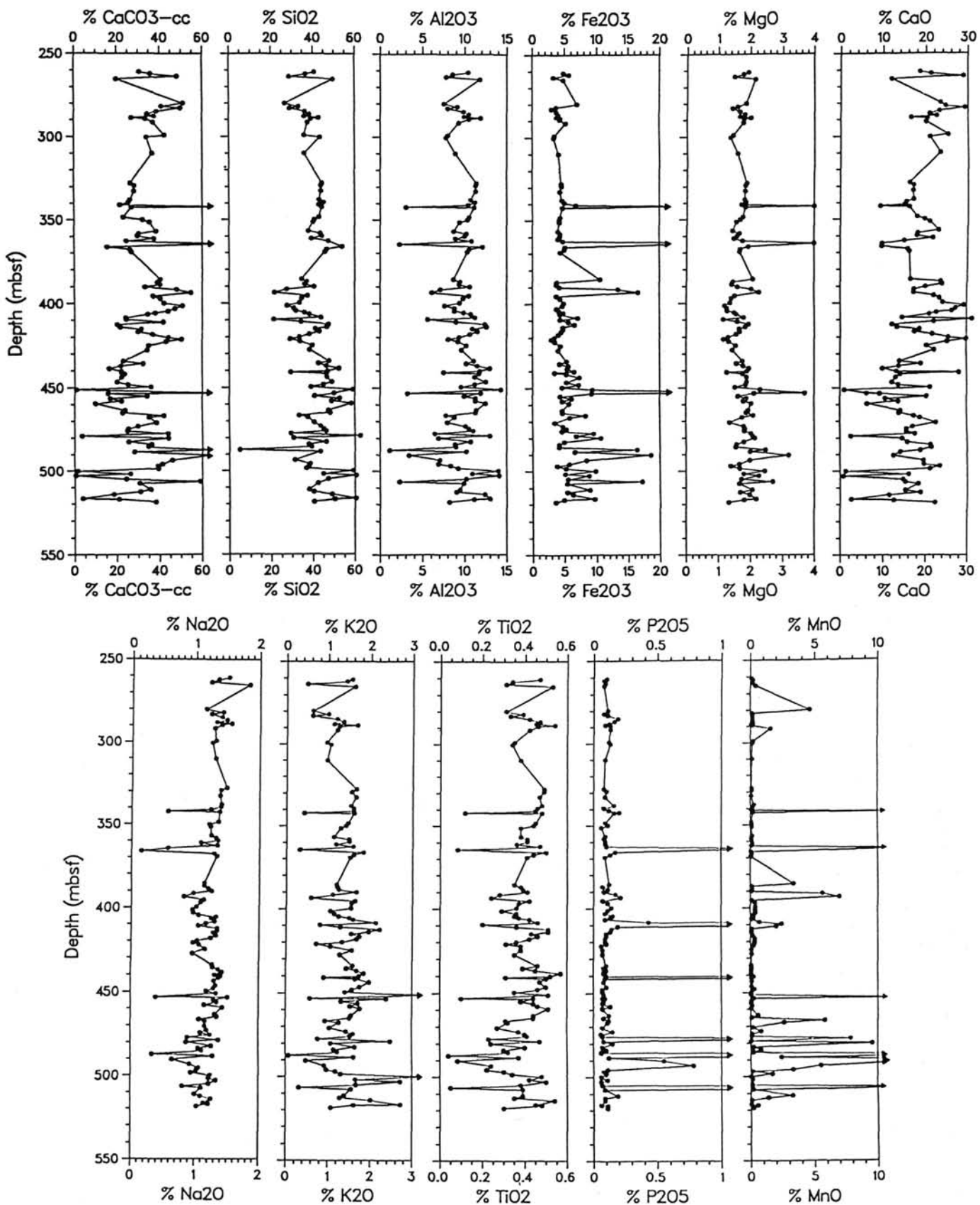


Figure 2. Concentrations of CaCO<sub>3</sub> computed from carbonate carbon (CC) and major-element oxides in samples from lithologic Unit IIIC, Hole 647A.

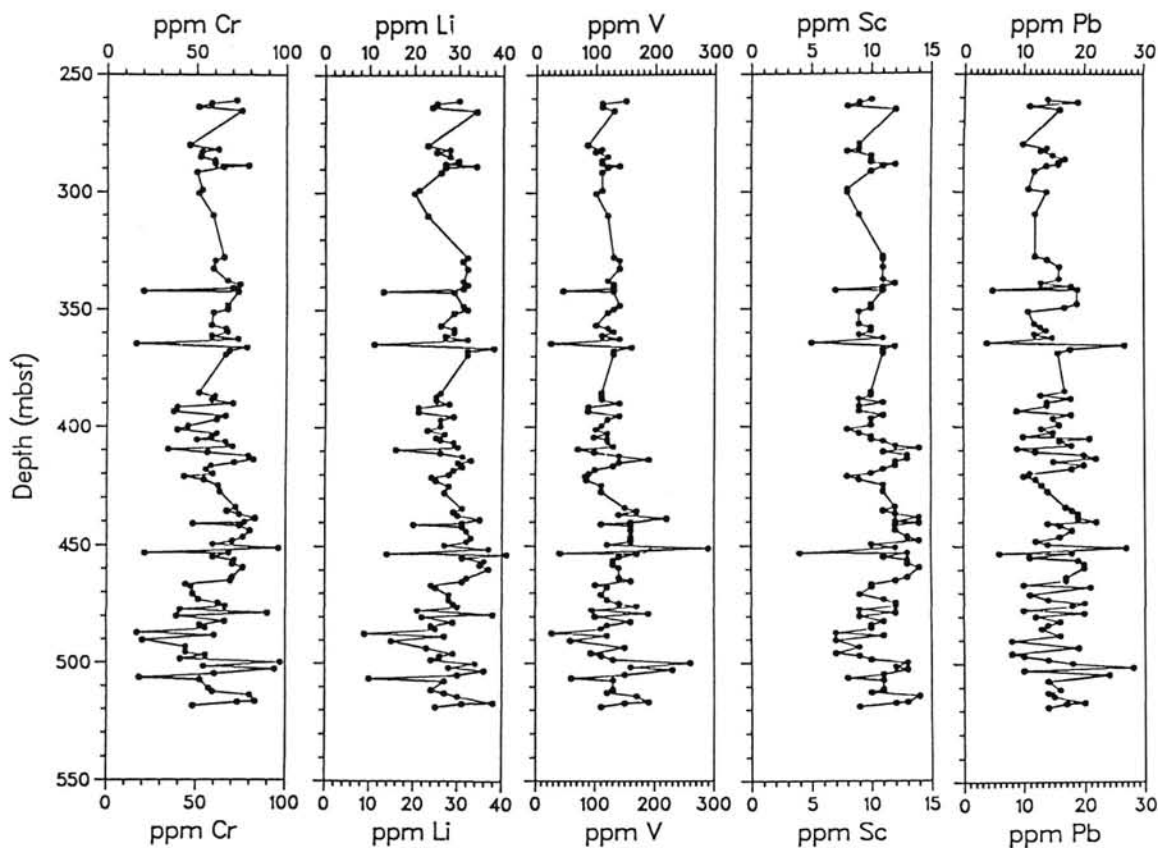


Figure 3. Concentrations of Cr, Li, Sc, and Pb in samples from lithologic Unit IIIC, Hole 647A.

tion of  $\text{CaCO}_3$  also can be calculated from the total Ca concentration ( $\text{CaCO}_3 = \text{Ca} \times 2.5$ ) with excellent agreement using  $\text{CaCO}_3$  concentration calculated from the CC concentration. Again, this assumption does not always work for the Site 647 samples.

Trace elements having downhole concentration patterns that are not obviously related to those of any other trace, minor, or major element include barium (Ba), thorium (Th), gallium (Ga), niobium (Nb), cobalt (Co), copper (Cu), nickel (Ni), and zinc (Zn) (Figs. 5 and 6).

To examine more objectively the relationships among elements and to determine groupings of samples based on their chemistry, we performed a Q-mode factor analysis using the extended CAB-FAC computer program of Klovan and Miesch (1976). Before conducting the factor analysis, concentrations of all oxides and elements were transformed to proportions of the total range for each oxide and element. As a result of the transformation, all data were expressed on a scale of 0.0 to 1.0. After trying several different sets of reference axes in multidimensional space and different numbers of reference axes, we finally chose four orthogonal reference axes that maximize the variance of the transformed data in each dimension (four-factor varimax solution). The four-factor model accounted for more than 60% of the variance in the scaled data for 22 elements, with an average of 92%. The four-factor model explained less than 30% of the variance in the scaled data for Ba, Co, Cu, Ga, Nb, Ni, Th, and Zn, which are the same elements that have unique downhole concentration patterns (Figs. 5 and 6). These eight elements were not included in the final Q-mode analysis. Basically, the four-factor Q-mode model reduced 22 measured variables (element concentrations plus LOI) to four "composite" geochemical variables. The intensities of the composite geochemical vari-

ables are the factor loadings. The loadings for each of the four factors are plotted vs. depth below seafloor in Figure 7.

The factor loadings describe the relative importance of each composite chemical variable (factor) for each sample, but give no indication of which elements had the most influence on determining each of the four factors. For example, Samples 43-4-25 (409.55 mbsf), 46-5-111 (440.91 mbsf), 51-4-68 (487.28 mbsf), and 53-4-79 (506.45 mbsf) have the highest loadings for factor II, and these samples are clearly different from all other samples, but the loadings do not indicate what actual geochemical characteristics (element concentrations) had the most influence on distinguishing these samples from the others. To determine which elements had the most influence on which factor, the factor loadings for each sample were treated as composite chemical variables, and correlation coefficients were computed between the loadings and the 23 observed compositional variables. Results of the correlation analysis are given in Table 2.

Table 2 shows that the elements that had the most influence on grouping samples in factor I are Al, Si, Cr, Ti, K, V, Li, Pb, Sc, and Na, in that order of importance (i.e., order of decreasing correlation coefficients). These are the elements that typically have a lithophile association (e.g., Goldschmidt, 1954); therefore, samples with high loadings for factor I have the greatest relative abundance of detrital clastic material.

Factor II is distinctly dominated by four samples, with moderate loadings for a few additional samples (Fig. 7), all in the lower one-half of lithologic Unit IIIC. Factor II samples are characterized by high concentrations of phosphorus and the REEs of Nd, Y, Ce, Yb, and La (Table 2).

Figure 7 shows that most samples have high loadings for factor III, which is the carbonate factor determined mainly by concentrations of Ca and Sr (Table 2). Factor IV, like factor II, is

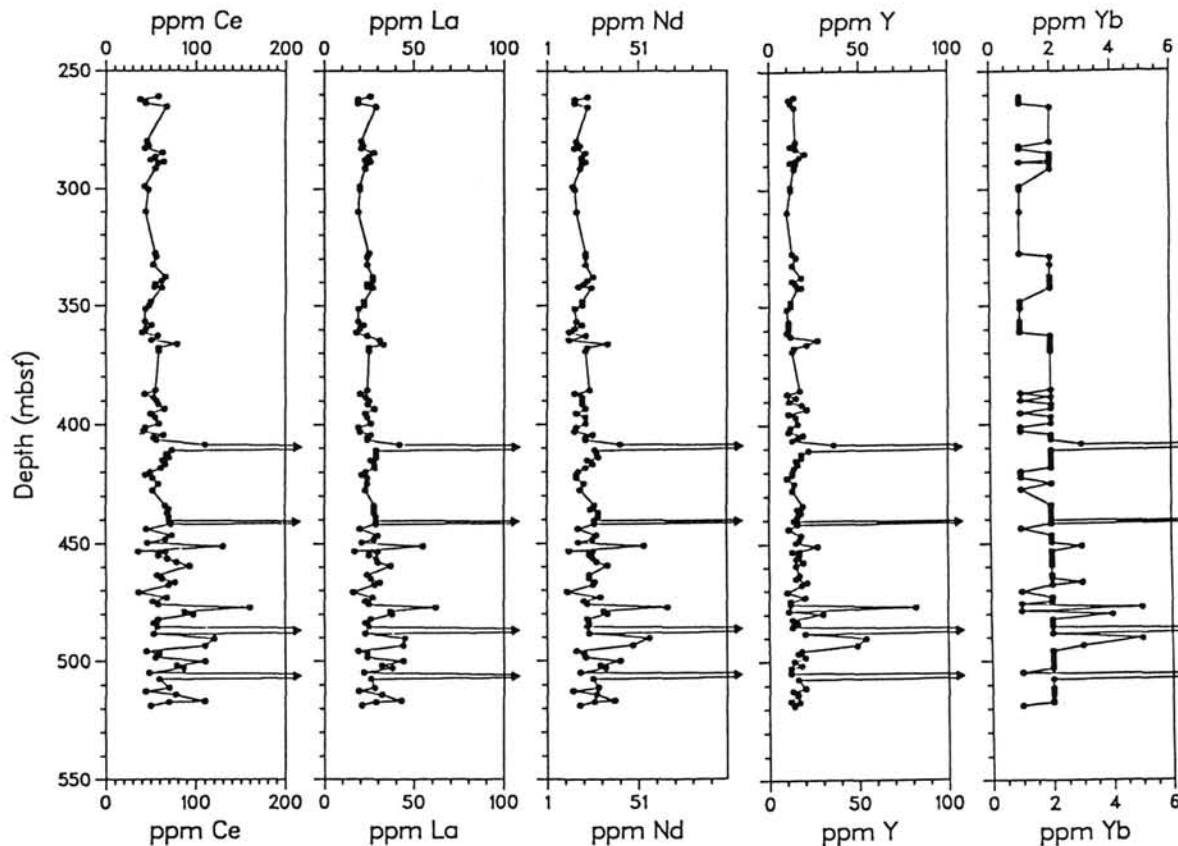


Figure 4. Concentrations of Ce, La, Nd, Y, and Yb in samples from lithologic Unit IIIC, Hole 647A.

dominated by four samples (although not the same four samples), with moderate loadings for a few other samples. The most important variables used to group factor IV samples are Mn, Fe, Mg, and LOI.

The raw data plots (Figs. 1 through 6), particularly the plots of factor loadings (Fig. 7), show that most samples from lithologic Unit IIIC consist mainly of detrital clastic material plus varying amounts of  $\text{CaCO}_3$ . That the clastic fraction is fairly typical of average crustal material is shown by Table 3, which compares the carbonate-free concentrations of elements in a typical sample from Unit IIIC (Sample 36-4-68) with those in average crust and average deep-sea clay. The most striking features of the downhole plots, however, are the horizons having distinctly different chemical characteristics because of high concentrations of one or more REE-bearing phosphate minerals and/or high concentrations of one or more Mn-, Fe-, and Mg-bearing minerals. Results of the Ca and CC analyses show that the phosphate mineral is indeed calcium phosphate (carbonate-fluorapatite as determined by X-ray diffraction [XRD], Tables 4 and 5) and the Mn-, Fe-, and Mg-bearing minerals are one or more phases of carbonate, which XRD analysis confirmed was rhodochrosite, siderite, and manganosiderite. We mentioned earlier that for most deep-sea carbonate sediments or rocks we obtain essentially identical results for the percentage of  $\text{CaCO}_3$  calculated from total Ca and from CC. For the Site 647 samples, however, neither method gives correct results for all samples because of excess Ca from the apatite and excess CC from Mn-Fe-Mg carbonate. The difference between the two methods is shown in Figures 8 and 9. Figure 9 is a downhole plot of  $\text{CaCO}_3$  computed from CC— $\text{CaCO}_3$  computed from Ca. The

differences plotted in Figure 9 and the analytical results can be used to calculate the amount of apatite present, and the amount and molar proportions of cations in the Mn-Fe-Mg carbonate. For example, Sample 43-4-25 (409.55 mbsf) contains 31.3%  $\text{CaO}$  (= 22.4% Ca), 14.8%  $\text{P}_2\text{O}_5$  (= 6.45% P), and 2.9% CC. Assuming that all of the P is in simple calcium fluorapatite ( $\text{Ca}_5\text{F}[\text{PO}_4]_3$ ) with a molar Ca:P ratio of 1.67, then 14.0% Ca is in apatite, and the amount of apatite in the sample is 35%. If all of the residual Ca (8.4%) is assumed to be in calcite, then the computed percentage of  $\text{CaCO}_3$  is 21%, which compares with 24% computed from CC.

As an example of a Mn-Fe-Mg carbonate, Sample 38-6-67 (364.6 mbsf) contains 31.5%  $\text{Fe}_2\text{O}_3$  (22% Fe), 12.9%  $\text{MnO}$  (10% Mn), 6.9%  $\text{CaO}$  (6.9% Ca), 1.6%  $\text{P}_2\text{O}_5$  (0.7% P), and 8.55% CC. Assuming that all of the P is in apatite with a Ca:P ratio of 1.67, and all of the residual Ca and all of the Mg, Mn, and Fe are in one carbonate mineral, then the formula for this carbonate mineral is:



Most of the other Fe- and Mn-rich samples have similar molar proportions of the four divalent cations.

The occurrence of these apparently authigenic carbonate and phosphate minerals seems anomalous for a primarily pelagic sedimentary sequence. However, the relatively high sedimentation rate (about 36 m/m.y.) over part of the sequence is more indicative of a hemipelagic regime, one in which suboxic to anoxic early diagenesis could induce substantial redistribution of organic-associated and redox-sensitive elements. In addition, there

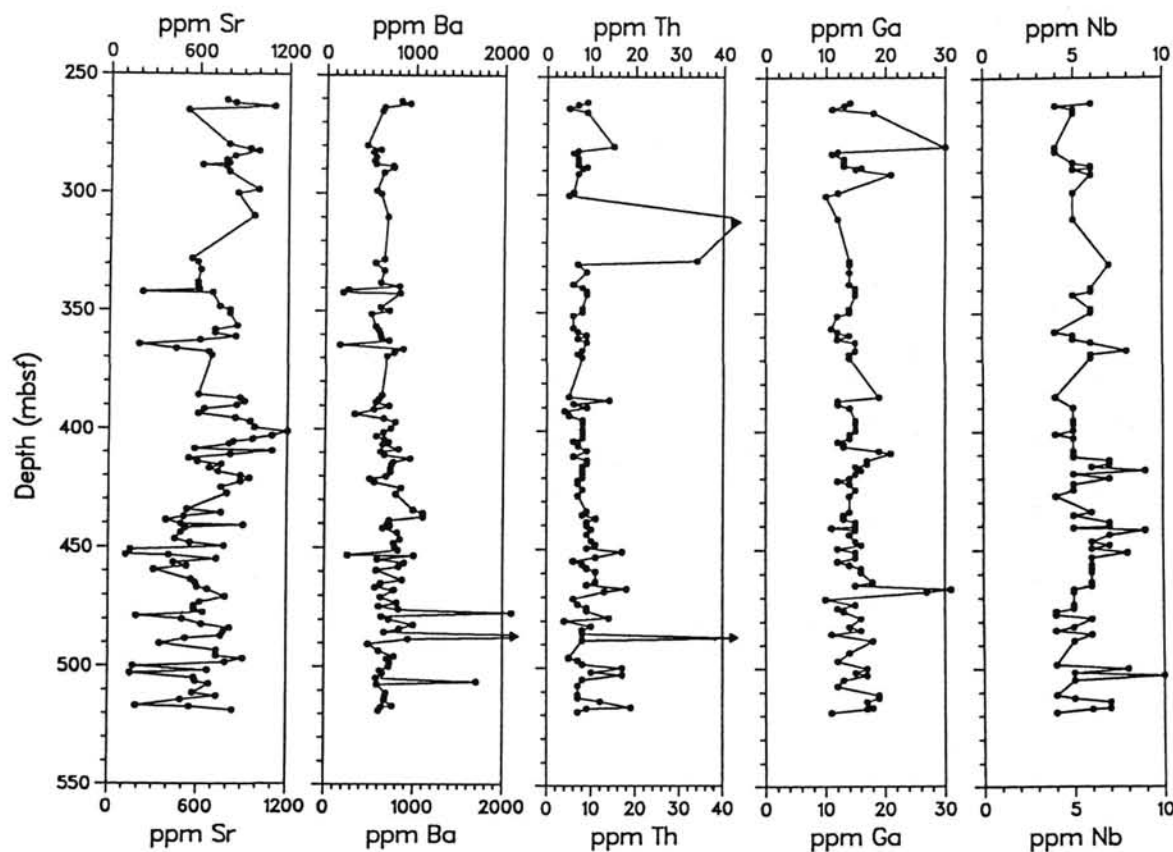


Figure 5. Concentrations of Sr, Ba, Th, Ga, and Nb in samples from lithologic Unit IIIC, Hole 647A.

is a potential for hydrothermal geochemical influx, at least in the lower part of the sequence. These possibilities are examined further in a later section of this chapter. Unfortunately, it is not possible to sort out the effects of diagenesis on primary geochemical signals related to paleoenvironment.

#### X-Ray Diffraction Results

Selected bulk samples, which had anomalous geochemical characteristics and which corresponded to levels of nodular or concretionary mineral layers, were analyzed using conventional XRD techniques (Table 5), as were a few of the "normal background" samples. The results generally confirm our inferences based on the geochemical data—specifically the elements Ca, Fe, Mn, Mg, P, and inorganic C. The most abundant authigenic carbonate phase is siderite or manganosiderite, typically characterized by broad peaks (Fig. 10), suggesting a phase intermediate in composition between siderite and rhodochrosite. No attempt was made to examine samples for compositional zoning because bulk sediment samples were ground for analysis. The broadened peaks possibly represent a number of discrete phases, with earliest precipitates having higher Mn contents and later precipitates having nearly pure siderite, as observed for some concretions from lower in the Eocene by Bohrmann and Thiede (this volume). Some samples consist of nearly pure siderite, but there appears to be no significant downcore trend in mineral dominance (Tables 4 and 5). In Cores 112-647A-43 and -46, nearly pure carbonate-fluorapatite concretions were detected on the basis of XRD (Fig. 10) and the anomalously high phosphate concentrations.

#### Stable Isotope Results

##### Oxygen Isotopes

Carbon and oxygen isotopic analyses were conducted on several species of benthic and planktonic foraminifers from a sequence at Site 647 spanning the late Eocene to early Oligocene. Results of these analyses are shown in Tables 6 and 7. Table 6 is a tabulation of visual preservation and abundance data for the samples selected for foraminifers.

Oxygen isotope values of planktonic foraminifers *Globigerina oeceanica* and *Catapsydrax unicavus* exhibit a slight enrichment of about 0.5‰ in values of  $\delta^{18}\text{O}$  from the middle Eocene to early Oligocene. *G. oeceanica* has  $\delta^{18}\text{O}$  values ranging from  $-1.80$  to  $-0.84\text{\textperthousand}$ , and *C. unicavus* is characterized by values of  $-1.84$  to  $-0.54\text{\textperthousand}$ . These  $\delta^{18}\text{O}$  values (Fig. 11) are in agreement with the oxygen isotope values of mixed planktonic foraminifers of the same age from nearby Site 112 (W. Curry and K. Miller, pers. comm., 1989). Similar but slightly greater enrichments have been reported at numerous other Eocene/Oligocene sequences worldwide and have been interpreted to represent either a global cooling of several degrees or an expansion of continental ice volume (e.g., Shackleton and Kennett, 1975; Keigwin, 1980; Keigwin and Corliss, 1986; Miller et al., 1987; Boersma et al., 1987).

No consistent difference exists in  $\delta^{18}\text{O}$  between *G. oeceanica* and *C. unicavus* at Site 647, in contrast to what was observed in low- to mid-latitude sequences (Keigwin and Corliss, 1986). This suggests either that the species maintained similar depth habitats, or as is the case for high latitudes in the modern ocean, the vertical temperature gradient in Labrador Sea surface waters

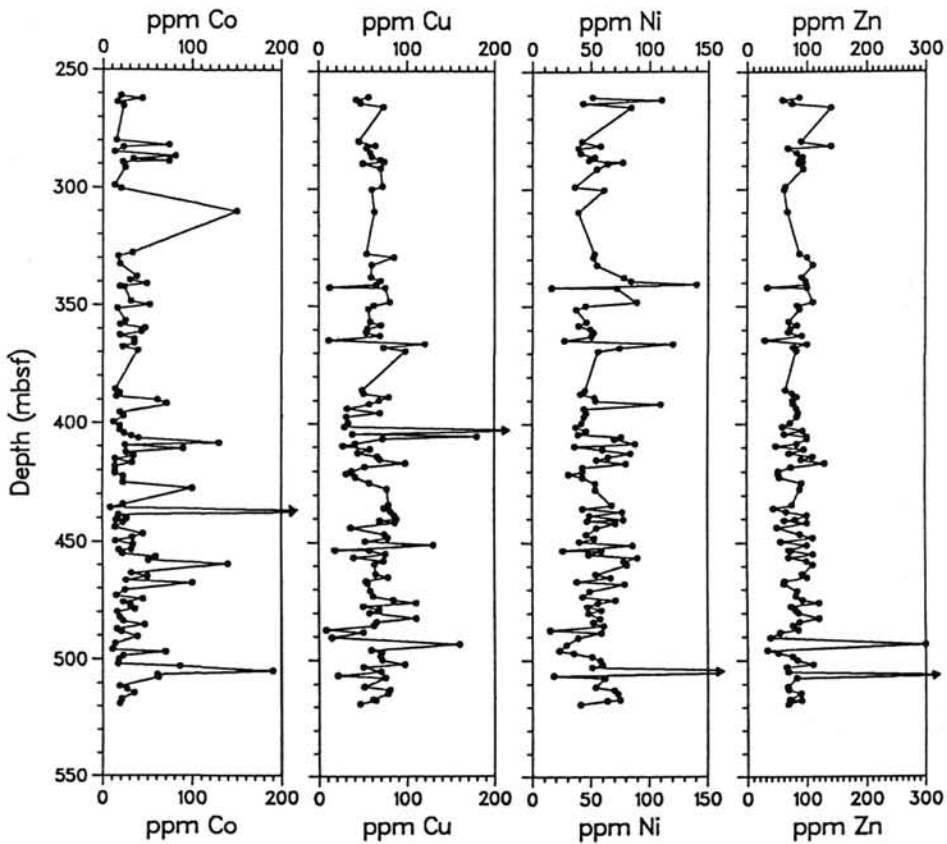


Figure 6. Concentrations of Co, Cu, Ni, and Zn in samples from lithologic Unit IIIC, Hole 647A.

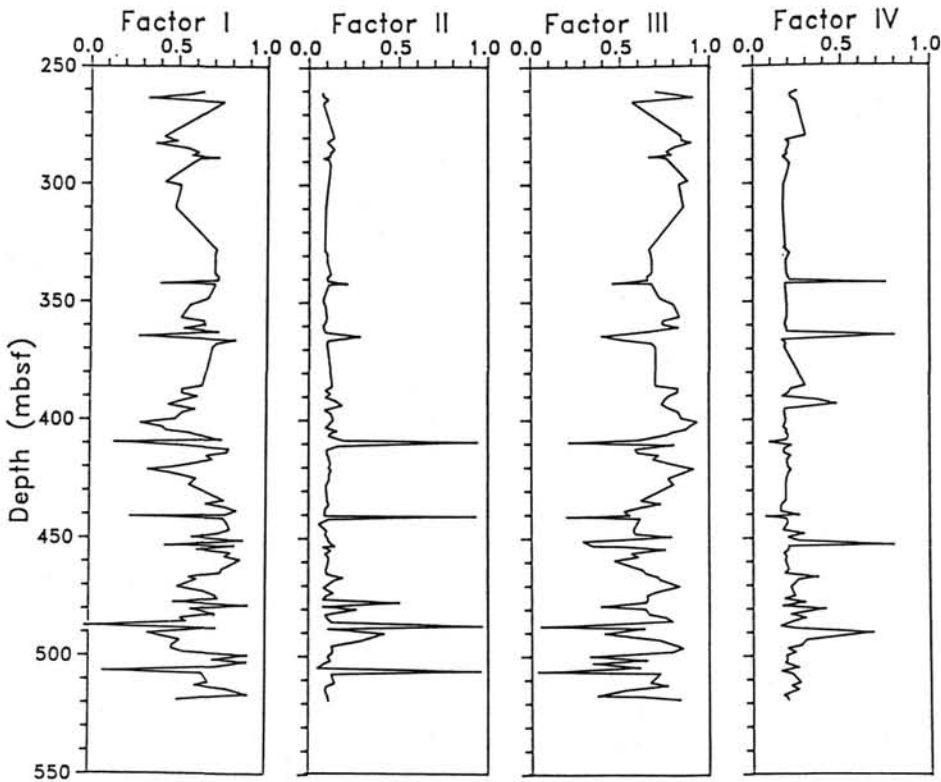


Figure 7. Plots of factor loadings from a four-factor Q-mode factor analysis of element concentrations in samples from lithologic Unit IIIC, Hole 647A.

**Table 2. Correlations between the factor loadings and the variables.**

	I	II	III	IV
SiO <sub>2</sub> %	0.8882	-0.6438	-0.1195	-0.1665
Al <sub>2</sub> O <sub>3</sub> %	0.8967	-0.6939	-0.0489	-0.1917
Fe <sub>2</sub> O <sub>3</sub> %	-0.2113	0.1085	-0.2944	0.9155
MgO %	-0.0893	0.0166	-0.2915	0.9087
CaO %	-0.5696	-0.1478	0.7765	0.2042
Na <sub>2</sub> O %	0.6597	-0.6406	0.0656	0.0581
K <sub>2</sub> O %	0.8468	-0.4933	-0.2978	-0.1563
TiO <sub>2</sub> %	0.8524	-0.6825	0.0196	-0.2559
P <sub>2</sub> O <sub>5</sub> %	-0.5525	0.8537	-0.5492	0.0547
MnO %	-0.3972	0.3067	-0.2944	0.9506
LOI 900°C	-0.4364	-0.1170	0.3408	0.8316
Ce ppm-s	-0.4014	0.8924	-0.7525	0.0458
Cr ppm-s	0.8570	-0.6365	-0.1236	-0.1810
La ppm-s	-0.3893	0.8281	-0.6882	0.0778
Li ppm-s	0.7828	-0.6665	-0.0816	0.1197
Nd ppm-s	-0.4244	0.9300	-0.7817	0.0106
Pb ppm-s	0.7718	-0.5601	-0.0733	-0.0771
Sc ppm-s	0.7054	-0.4589	-0.2454	0.2433
Sr ppm-s	-0.4405	-0.2691	0.8864	-0.0989
V ppm-s	0.8234	-0.5115	-0.2417	-0.1494
Y ppm-s	-0.5560	0.9280	-0.6184	0.0519
Yb ppm-s	-0.4786	0.8808	-0.6685	0.2118

**Table 3. Concentrations of major-element oxides and trace elements in average upper continental crust (Wedepohl, 1971), average deep-sea clay (Chester and Aston, 1976), red clay from the Bermuda Rise (V26-157), carbonate-free Sample 105 647A-36R-4, 68 cm, and average background sediments ( $n = 99$ ) from Site 647.**

	1 Avg. Crust	2 Deep-Sea Clay	3 V26-157	4 36-4-68 (carb.-free)	5 Avg. Bkgrd. (n = 99) (carb.-free)
<b>Oxide (%)</b>					
SiO <sub>2</sub>	65.3	60.4	53.5	62.4	62.1
Al <sub>2</sub> O <sub>3</sub>	14.8	19.1	18.9	15.6	15.2
Fe <sub>2</sub> O <sub>3</sub>	5.06	8.93	8.15	6.6	7.3
MgO	2.30	3.73	2.88	2.6	2.5
Na <sub>2</sub> O	3.29	1.67	2.02	1.9	1.9
K <sub>2</sub> O	3.38	3.56	3.96	2.3	2.2
TiO <sub>2</sub>	0.71	0.92	0.84	0.68	0.61
P <sub>2</sub> O <sub>5</sub>	0.19	0.16	0.16	0.23	0.17
MnO	0.09	0.52	0.14	0.27	0.60
<b>Element (ppm)</b>					
Ba	590	2300	503	1170	1050
Co	12	74	26	34	58
Cr	70	90	89	100	94
Cu	30	250	42	110	100
Ga	17	20	31	21	—
La	44	115	50	38	38
Li	30	57	94	41	43
Nb	14	—	7	8	—
Nd	140	—	35	34	—
Ni	44	225	58	100	89
Pb	15	80	20	27	23
Sc	14	19	19	15	16
Th	11	5	—	13	13
V	60	120	127	180	200
Y	34	9	27	23	22
Yb	15	—	3	—	2.5
Zn	60	165	120	140	130

was minimal at this time. Converting the oxygen isotope values to paleotemperature would indicate a range of 16° to 20°C for the Labrador Sea, depending on whether ice-free conditions are assumed. Although broken shells are common, visual and scanning electron microscope (SEM) examination showed that the preservation of the planktonic foraminifer shells was good, with little or no sign of infilling and/or external overgrowth.

**Table 4. Abundance of concretionary intervals in Cores 105-647C-28 through -54, estimated from core photographs.**

Core number	No. of concretion zones	Core recovery (m)	Avg. and total thickness concretion zone	Sediment that is concretion (%)
29	0	6.0	—	0
30	2	9.5	(1 cm) 2	0.22
31	1	2.7	(1 cm) 1	0.37
32	1	2.0	(0.5 cm) 0.5	0.25
33	0	2.4	—	0
34	0	1.5	—	0
35	1	5.2	(4.0 cm) 4	0.77
36	2	6.0	(2 cm) 4	0.67
37	2	5.65	(2 cm) 4	0.70
38	5	9.5	(3 cm) 15	1.60
39	0	4.0	—	0
40	0	0.25	—	0
41	6	8.7	(1.8 cm) 11	1.30
42	4	9.7	(3.8 cm) 15	1.55
43	0	9.5	—	0
44	0	8.7	—	0
45	0	4.3	—	0
46	0	9.0	—	0
47	0	8.0	—	0
48	1	8.5	(10 cm) 10	1.18
49	7	9.5	(2.1 cm) 14.5	1.53
50	12	9.0	(1.6 cm) 19	2.11
51	13	9.0	(1.7 cm) 21.5	2.39
52	9	6.5	(1.5 cm) 13.5	2.10
53	9	7.2	(1.6 cm) 14	1.94
54	8	8.0	(1.25 cm) 10	1.25

In contrast to the planktonic foraminifers, benthic foraminifers from the lower Eocene to lower Oligocene interval yield a much wider range of  $\delta^{18}\text{O}$  values. Samples of *Oridorsalis* species and *Globocassidulina subglobosa* from about 285 mbsf near the Eocene/Oligocene boundary yield  $\delta^{18}\text{O}$  values of 0.28 to 0.72‰. These values are also similar to those recorded for *Gyroidinoides* species from early Oligocene cores of Site 112 (Curry and Miller, unpub. data) as well to values for benthic foraminifers of similar age from other Atlantic locations (Miller et al., 1987; Keigwin and Corliss, 1986). However, farther below, in the upper Eocene part of the sequence, a progressive downcore depletion occurs in the oxygen isotopic values of the benthic foraminifers. From 285 to 400 mbsf, the  $\delta^{18}\text{O}$  of both *Oridorsalis* species and *Cibicidoides* decrease by more than 4‰. Other species of benthic foraminifers, *Nuttallides truemeyi*, *G. subglobosa*, and *Stilostomella* exhibit similar depletions, although not so large.

A puzzling aspect of these more negative oxygen-isotope values is that the  $\delta^{18}\text{O}$  values of planktonic foraminifers remain more-or-less constant throughout the interval in which the values of benthic foraminifers decline. If interpreted in terms of temperature, the negative  $\delta^{18}\text{O}$  gradient from surface to bottom would imply an inverted density gradient, with much warmer bottom waters. Because these environmental conditions seem unreasonable, differential diagenesis must be responsible for the observed isotopic trends. The depleted values of the benthic foraminifers indicate that recrystallization, or carbonate cementation, may have occurred within the benthic foraminiferal tests. Visual examination of the benthic foraminifers revealed some signs of carbonate overgrowths, but most samples are reasonably well-preserved (moderate to good). The planktonic foraminifers display few signs of cement overgrowth. Why such selective diagenesis occurred is unclear at this time. The tests of benthic foraminifers tend to be more robust and coarsely crystalline; whereas, tests of calcareous nannofossils and planktonic foraminifers are generally more porous, fine-grained, and solution susceptible. If substantial dissolution/recrystallization did occur,

Table 5. Whole-sediment (concretions or layers) XRD results.

Core/section/ interval	Depth (mbsf)	Main minerals present	Comments	Fe <sub>2</sub> O <sub>3</sub> , MnO, P <sub>2</sub> O <sub>5</sub> (%)
105-647A-30-1, 51	279.93	Siderite-Rhodochrosite-Calcite		(not anomalous)
36-4, 42	342.13	Siderite-Manganosiderite	(broad peaks)	(31.5, 11.5, 0.21)
38-6, 67	364.56	Siderite-Manganosiderite	(broad peaks)	(31.5, 12.9, 1.56)
43-4, 25	409.55	Aparite-Calcite		(4.31, 2.42, 14.8)
46-5, 111	440.91	Aparite		(3.46, 0.23, 11.3)
48-1, 7	453.27	Siderite-Manganosiderite	(sharp peaks)	(37.2, 11.5, 0.55)
50-4, 32	477.32	Siderite-Rhodochrosite-Calcite		(9.5, 7.86, 2.01)
51-4, 68	487.28	Rhodochrosite-Siderite	(broad peaks)	(16.4, 20.2, 7.31)
51-6, 83	490.43	Siderite-Rhodochrosite-Calcite	(Calcite peak shift; Mg substitution)	(18.6, 15.5, 0.55)
52-2, 10	493.40	Calcite-(minor) Siderite		(not anomalous)
53-4, 79	506.45	Manganosiderite		(17.2, 16.7, 7.6)

Note: Diffractometer parameters:  $1.2^\circ 2\theta/\text{min}$  from 10 to  $60^\circ 2\theta$  with CuK $\alpha$  radiation.

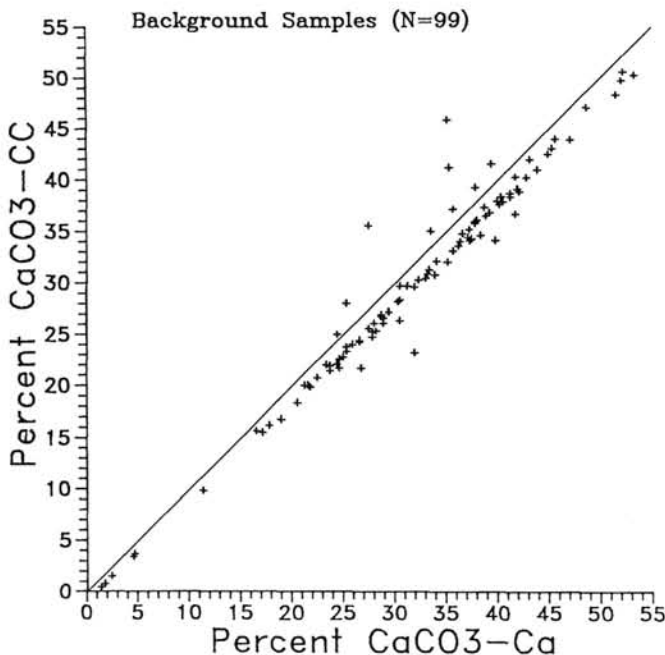


Figure 8. Plot of CaCO<sub>3</sub> of "background" (nonconcretionary) samples from Hole 647A calculated from carbonate carbon (coulometry, see text) vs. that calculated from Ca geochemical data. Note close agreement between two techniques, with the exception of a few points, which probably contain authigenic carbonate phases.

cur, the solution-susceptible planktonic tests may be the primary source of carbonate, while the interior and exterior walls of benthic tests are the selective sites for cement precipitation. Of the benthic foraminifers, *Oridorsalis* species and *Cibicidoides* consistently display the lightest values, suggesting that of the benthics these species provide the most favorable sites for cement precipitation.

#### Carbon Isotopes

As with the oxygen isotopes, the carbon isotopic composition of the planktonic foraminifers is little affected by diagenesis. Samples of both *C. unicavus* and *G. eoceanus* have  $\delta^{13}\text{C}$  values of 0.50 to 0.75‰ from the middle Eocene, again with no discernable difference between the species. A slight decrease in  $\delta^{13}\text{C}$  can be measured from the middle to upper Eocene parts of the seafloor, where the average values of planktonic foraminifers are less than 0.25‰ (Fig. 11).

The carbon isotopic composition of the benthic foraminifers is progressively more negative from lower to upper Eocene at

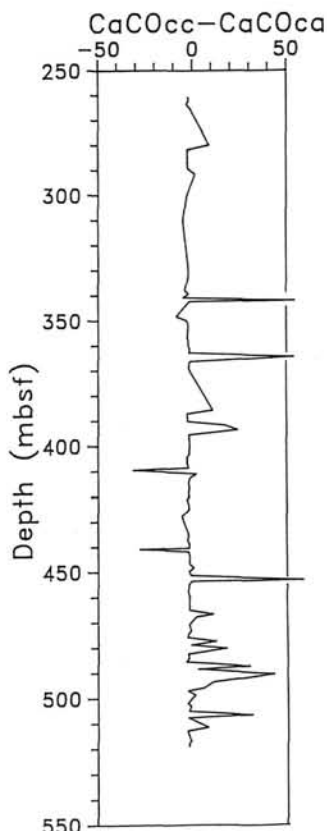


Figure 9. Plot of difference in CaCO<sub>3</sub> computed from carbonate carbon (CC) and from calcium for samples from lithologic Unit IIIC, Hole 647A.

Site 647 (Fig. 11). The measured  $\delta^{13}\text{C}$  values for all species range from  $-0.7$  to  $+0.5\text{\textperthousand}$  in the lower Eocene and from  $-2.0$  to  $-0.3\text{\textperthousand}$  in the upper Eocene, with *Oridorsalis* consistently yielding the lightest values. The carbon isotopic compositions of *Nuttallides* and *Cibicidoides* overlap upsection and are on average 1.0‰ heavier than those of *Oridorsalis*.

Comparatively heavier  $\delta^{13}\text{C}$  values, in the range of  $-0.25$  to  $1.5\text{\textperthousand}$ , have been reported for various species of benthic foraminifers from other Eocene pelagic sequences located in the equatorial Pacific (Keigwin, 1980), south Atlantic, eastern Indian Arabian Sea (Keigwin and Corliss, 1986), and the Bay of Biscay (Miller et al., 1985). In addition, the records at these locations give no indication of a depletion in the deep-water mass carbon isotopic composition during the middle to late Eocene.

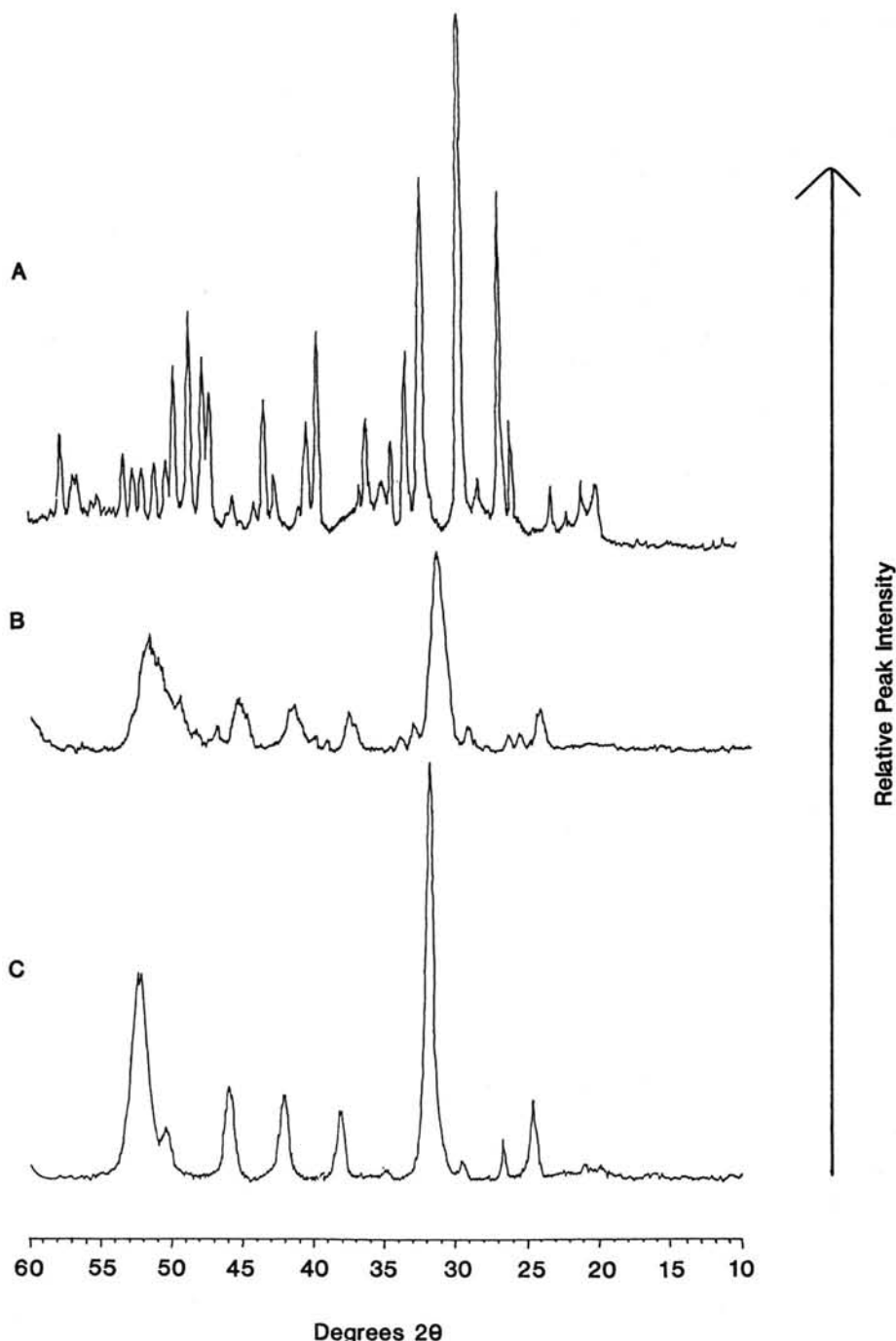


Figure 10. Representative X-ray diffractograms of three different concretionary phases. A. Sample 105-647A-46R-5, 111 cm: all sharp peaks indicate pure carbonate fluorapatite phase. B. Sample 105-647A-51R-4, 68 cm: broadened peaks suggest composition intermediate between rhodochrosite and siderite (i.e., manganosiderite) or a range of Fe-Mn carbonates in bulk samples. C. Sample 105-647A-48R-1, 7 cm: sharp peaks mainly siderite, with some manganese substitution, but no discrete rhodochrosite.

This discrepancy may arise from one of several factors as outlined below.

The interstitial waters of the upper few centimeters of the substrate at this particular location could have been characterized by substantially lighter carbon isotope compositions. Benthic foraminifers inhabiting shallow levels in the sediment could then have precipitated carbonate in equilibrium with a lighter total dissolved carbon source. This would have occurred if the

amount of isotopically light OC accumulating and decaying within the substrate were higher here than elsewhere (e.g., McCorkle, 1987). Productivity (OC flux), sedimentation rate, and/or the oxygen levels of the deep-water mass all have a bearing on the preservation of OC in the sediments. It is difficult to determine which of these parameters exerted the greatest influence of OC accumulation rates here, but sedimentation rate may have had the most influence. Neither carbonate nor biogenic opal ac-

Table 6. Visual (microscopic) estimation of preservation of samples picked for benthic and planktonic foraminifers for stable-isotope analyses.

Core, section interval (cm)	Depth (mbsf)	Benthic preservation	Comments	Planktonics
105-647A-28-1, 108-115	261.18	G		
28-2, 105-108	262.65	G		
28-3, 105-108	264.15	G		
28-4, 91-98	265.51	G		
28-4, 105-108	265.65	G		
30-1, 107-111	280.47	G		Few dwarf
30-2, 25-29	281.15	G		G
30-3, 110-114	283.54	G		G
30-4, 107-111	284.97	M/G	(Few pits, pyrite)	Few
30-5, 10-12	285.50	M/G	(Some etching, <i>Nuttalides</i> abundant)	
30-7, 33-38	288.73	M/G	(Some pyrite in- <i>Orid.</i> )	M/G
31-1, 132-136	299.92	M/G	(Signs of etching)	
31-2, 34-37	290.84	M/G	(Some etching)	
32-1, 84-93	299.44	M	(Stronger etching, <i>Orid.</i> /pyrite)	M
32-2, 20-24	300.30	M/G	(Some etching, <i>Gyrodin.</i> )	
33, CC	310.60	M/G	(No pyrite, some etching)	
34, CC	319.30	M/G	(No visible pyrite)	
35-1, 77-80	328.37	M/G	(Abund. pyrite on all forms)	
35-2, 77-80	329.87	M	(Pyrite; etching; broken spec.)	M/G
35-3, 77-80	331.37	M/G	(Better than above, no pyrite)	
36-2, 49-52	339.19	M	(Abund. pyrite, etching)	M low abund.
36-3, 49-52	340.69	M/G	(No pyrite, better than above)	
36-4, 49-52	342.19	M/G	(Pyrite present)	
37-2, 90-93	349.10	M	(Abund. pyrite)	
37-3, 90-93	350.60	P/M	(Abund. pyrite, etching frags.)	low abund.
37-4, 90-93	352.10	M/G	(Pyrite absent)	
38-1, 83-86	357.24	M	(Orange; some etching)	M/G abund.
38-2, 84-87	358.74	M/G	(Orange)	
38-3, 86-89	360.26	M/G	(Clear/White)	
38-4, 86-89	361.76	M/G	(No pyrite/clear)	
39-1, 80-83	366.90	M	(Orange/pyrite)	
39-2, 77-80	368.37	M/G	(Low abund., trace pyrite)	M (w/ppm)
39, CC	370.10	M	(Orange; pyrite abund.)	M (some pyr.)
41-1, 58-61	385.98	M/G	(White, some pyrite)	
41-3, 58-61	288.98	M	(White, no pyrite)	M/G
41-5, 58-61	391.98	M/G	(White, no pyrite)	
42-3, 32-35	398.42	M/G	(White, no pyrite)	
42-5, 96-100	402.06	M/G	(White, no pyrite)	
43-1, 95-98	405.75	M	(White, no pyrite)	
43-3, 104-108	408.84	M	(Some etching, no pyrite, white)	M/G
43-5, 97-100	411.77	M	(Dissolved, some pyrite)	
44-1, 45-48	414.95	M/G	(Some pyrite)	M/G
44-3, 42-46	417.92	M/G	(No pyrite)	
44-5, 45-48	420.95	G	(No pyrite, white, clear)	
45-1, 14-18	424.24	M/G	(No pyrite, some etching)	
45-2, 20-24	425.80	M/G	(No pyrite, some etching)	
46-1, 60-63	434.40	M	(Orange color, no pyrite)	
46-3, 60-63	437.40	M	(Orange color, no pyrite)	
46-5, 60-63	440.40	M	(Orange color, abund. pyrite)	
47-4, 74-74	448.74	M/G	(No pyrite, white)	
47-5, 55-58	450.05	M/G	(No pyrite, orange)	
47-6, 52-55	451.52	P	(Nearly barren)	
48-1, 100-109	454.20	M	(Orange, no pyrite)	
48-3, 107-110	457.27	M	(Orange, some pyrite)	M
48-5, 104-107	460.24	M	(Lt. orange, some pyrite)	
49-1, 118-121	463.98	M/G	(White, no pyrite)	
49-5, 117-120	469.97	M/G	(Orange tinge, white, no pyrite)	
49-6, 117	471.47	M/G	(White, no pyrite)	
50-1, 91-94	473.41	M/G	(Some pyrite, orange)	
50-3, 91-94	476.41	M	(White, no pyrite)	M
50-5, 44-46	478.94	M/G	(White, no pyrite)	
51-2	493.60	M	(Orange tinge, trace pyrite)	
51-4, 69-71	487.29	M/G	(Orange tinge, trace pyrite)	
51-5, 94-97	489.04	M/G	(Orange tinge, low abund., no pyrite)	
52-2, 45-48	493.75	M/G	(Orange tinge, low abund., no pyrite)	
52-3, 45-48	495.25	M	(Trace pyrite, white)	
52-5, 52-55	498.32	M/G	(White, no pyrite)	
53-2, 40-44	503.30	M	(Some pyrite, white)	
53-4, 84-87	505.24	M/G	(Orange, no pyrite)	
53-5, 24-26	507.74	M	(Slight orange tinge, no pyrite)	
54-2, 32-35	512.82	M	(Slight orange tinge, trace pyrite)	
54-6, 23-27	518.83	M/G	(White, no pyrite)	

Table 6 (continued).

Core, section interval (cm)	Depth (mbsf)	Benthic preservation	Comments	Planktonics
105-647A-55, CC	521.10	M/G	(White, no pyrite)	
56, CC	530.40	M/P	(Orange, pyrite)	
58, CC	549.80	M	(Low abund. orange, pyrite)	
59, CC	559.60	M	(Low abund. orange, pyrite)	
60, CC	577.20	M	(Orange tinge, trace pyrite)	
61, CC	588.40	M/G	(White, trace pyrite)	
62-1, 112-115	599.22	M/G	(White, no pyrite)	
62-3, 60-63	601.70	M/G	(White, no pyrite)	
62-6, 22-2	605.82	M/G	(White, abund. pyrite)	
63, CC	610.20	Barren		
66-2,	638.30	G	(White)	
66-3,	639.80	M	(White)	
66, CC	640.50	M	(Pyrite, orange)	
67-1	646.50	G	(Pyrite, orange)	
67-3	649.50	Barren		
67, CC	651.20	Barren		
68-1	656.20	G	(White, no pyrite)	
68-3, 74-77	659.94	G	(White, no pyrite)	
70-2	686.70	Silicified to base of hole		

G = good; M = moderate; P = poor.

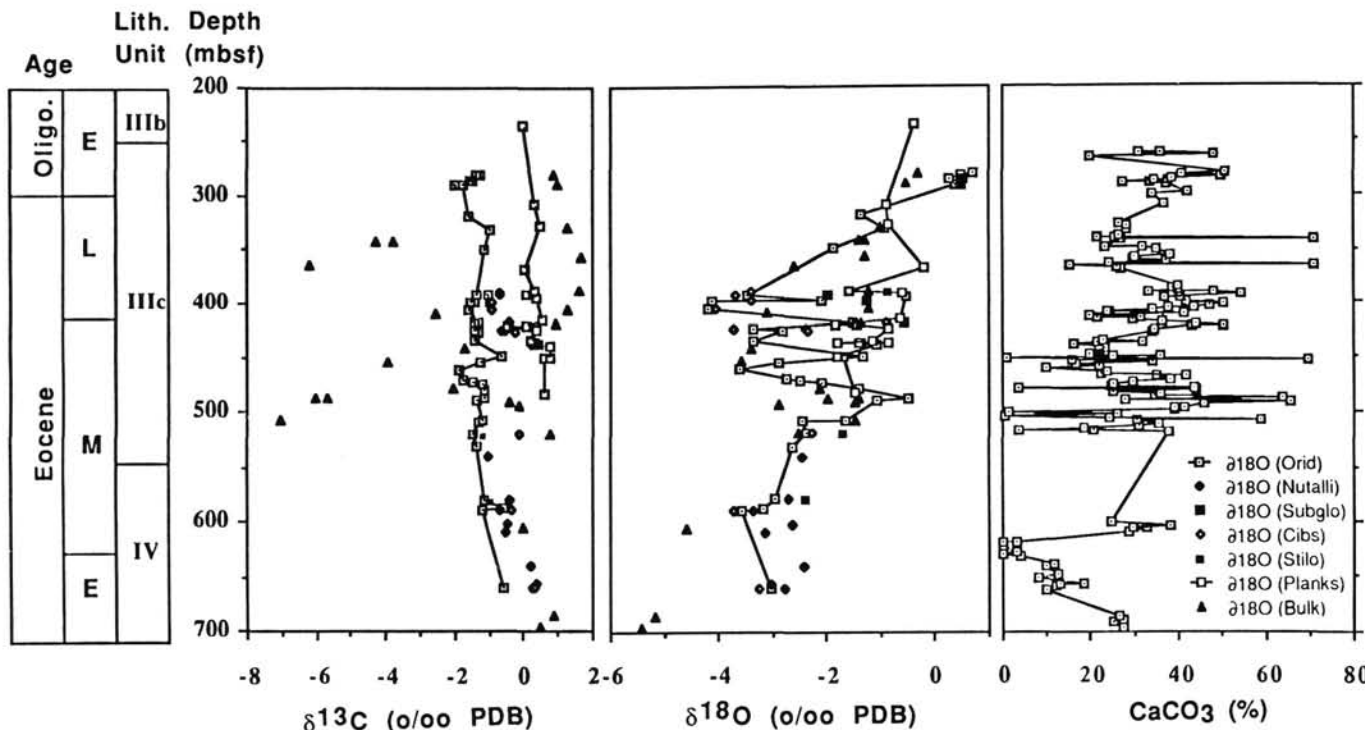


Figure 11. Stable isotope data, discrete planktonic and benthic foraminifer separates, and whole-rock samples (see key and Table 7) from Hole 647A.

cumulation rates are excessively high in the Eocene sequence, indicating that primary production may not have been particularly high. The average sedimentation rates for the Eocene and Oligocene at Site 647, however, exceed 36 m/m.y., a relatively high rate. This may have enhanced the initial amounts of OC buried here (e.g., Müller and Suess, 1979), in comparison with other regions having similar OC rain rates but lower rates of sediment accumulation. As for the deep-water mass paleo-oxygen levels, the substantial numbers of agglutinated benthic foraminifers suggest that concentrations were low (see Kaminski et

al., this volume). If so, the oxidation of OC before burial may have been somewhat reduced.

An alternative, or possibly complementary, explanation for the more negative carbon compositions, is that the  $\delta^{13}\text{C}$  values of the benthic foraminifers were altered during diagenesis. This would require that during the process of dissolution/recrystallization, a source of isotopically light dissolved carbon (derived from degradation of OC) be present. The diagenetic process could have occurred soon after burial when significant quantities of OC were still available, but the lighter oxygen-isotope

**Table 7.** Stable-isotope results from planktonic and benthic foraminifers and bulk samples.

Core, section, interval (cm)	Species	Depth (m)	$\delta^{18}\text{O}$ (PDB)	$\delta^{13}\text{C}$ (PDB)
105-647A-25-2, 28-30	<i>Unicavus</i>	233.80	-0.38	-0.01
33cc	Mixed plankton	308.30	-0.90	0.30
35cc	Mixed plankton	327.60	-0.84	0.46
39-2, 16-18	<i>Eoceanus</i>	367.60	-0.21	0.01
41-3, 29-31	<i>Unicavus</i>	388.69	-1.58	0.29
41-5, 29-31	<i>Unicavus</i>	391.69	-0.59	0.09
42cc	Mixed plankton	395.10	-0.54	0.39
44-1, 79-81	<i>Unicavus</i>	415.29	-0.63	0.53
44-4, 115-117	<i>Eoceanus</i>	420.15	-1.44	-0.45
44-4, 115-117	<i>Unicavus</i>	420.15	-1.84	0.07
45cc	Mixed plankton	424.10	-0.85	0.37
46cc	Mixed plankton	433.80	-1.15	0.23
46-2, 40-42	<i>Unicavus</i>	435.50	-1.41	0.34
46-2, 40-42	<i>Eoceanus</i>	435.50	-1.78	0.26
46R, 2	<i>Unicavus</i>	436.80	-1.37	0.30
46R, 2	<i>Eoceanus</i>	436.80	-0.84	0.41
46-3, 40-42	<i>Unicavus</i>	437.20	-1.36	0.39
46-4, 40-42	<i>Unicavus</i>	438.70	-1.06	0.74
47-5, 20-22	<i>Unicavus</i>	449.70	-1.67	0.58
47-5, 20-22	<i>Eoceanus</i>	449.70	-1.80	0.75
51cc	<i>Eoceanus</i>	482.10	-1.46	0.57
30-1, 107-109	<i>Oridorsalis</i>	280.47	0.72	-1.39
30-2, 25-27	<i>Oridorsalis</i>	281.15	0.49	-1.25
30-4, 107-109	<i>Oridorsalis</i>	284.97	0.28	-1.56
30-4, 107-109	<i>G. Subglobosa</i>	284.97	0.52	-1.46
31-1, 132-134	<i>Oridorsalis</i>	290.32	0.39	-1.76
31-1, 132-134	<i>G. Subglobosa</i>	290.32	0.49	-1.98
33cc	<i>Oridorsalis</i>	318.00	-1.35	-1.61
35-3, 77-79	<i>Oridorsalis</i>	331.37	-0.92	-0.97
36-2, 49-51	<i>Oridorsalis</i>	349.19	-1.86	-1.16
41-3, 58-61	<i>Cibicidoides</i>	388.98	-3.38	-0.71
41-3, 58-61	<i>Stilostomella</i>	388.98	-0.84	-0.62
41-5, 58-60	<i>Oridorsalis</i>	391.98	-3.47	-1.39
41-5, 58-60	<i>G. Subglobosa</i>	391.98	-1.96	-1.05
41-5, 58-61	<i>Cibicidoides</i>	391.98	-3.67	-0.70
42-3, 32-34	<i>Oridorsalis</i>	398.42	-2.07	-1.53
42-3, 32-34	<i>G. Subglobosa</i>	398.42	-1.24	-0.96
42-3, 33-35	<i>Cibicidoides</i>	398.43	-3.38	-0.90
41-3, 58-61	<i>Oridorsalis</i>	398.98	-4.13	-1.45
43-1, 95-97	<i>Oridorsalis</i>	405.75	-4.19	-1.61
43-1, 95-98	<i>Cibicidoides</i>	405.75	-4.04	-0.94
44-3, 24-26	<i>Oridorsalis</i>	417.74	-1.50	-1.31
44-3, 24-26	<i>G. Subglobosa</i>	417.74	-0.56	-1.42
44-3, 42-46	<i>Cibicidoides</i>	417.92	-0.88	-0.40
45-1, 14-16	<i>Oridorsalis</i>	424.24	-3.34	-1.43
45-1, 14-16	<i>Nuttallides</i>	424.24	-2.36	-0.62
45-1, 14-18	<i>Cibicidoides</i>	424.24	-3.71	-0.52
45-2, 20-22	<i>Oridorsalis</i>	425.80	-2.81	-1.33
45-2, 20-24	<i>Cibicidoides</i>	425.80	-2.34	-0.22
46-1, 60-62	<i>Oridorsalis</i>	434.40	-3.36	-1.43
47-5, 55-57	<i>Oridorsalis</i>	448.65	-1.32	-0.63
48-1, 106-108	<i>Oridorsalis</i>	454.26	-2.88	-1.28
48-5, 104-106	<i>Oridorsalis</i>	460.24	-3.61	-1.89
49-5, 117-119	<i>Oridorsalis</i>	469.97	-2.72	-1.76
49-6, 117-119	<i>Oridorsalis</i>	471.47	-2.48	-1.51
50-1, 91-93	<i>Oridorsalis</i>	473.41	-2.10	-1.22
50-5, 44-46	<i>Oridorsalis</i>	478.94	-1.39	-1.12
51-4, 69-71	<i>Oridorsalis</i>	487.29	-0.48	-1.17
51-5, 49-51	<i>Oridorsalis</i>	488.59	-1.08	-1.36
53-4, 84-87	<i>Oridorsalis</i>	506.74	-1.66	-1.21
53-5, 24-26	<i>Oridorsalis</i>	507.64	-2.43	-1.34
54-6, 23-27	<i>Oridorsalis</i>	518.83	-2.36	-1.48
54-6, 23-27	<i>Stilostomella</i>	518.83	-1.69	-1.13
54-6, 24-27	<i>Cibicidoides</i>	518.84	-2.25	-0.12
55cc	<i>Oridorsalis</i>	530.30	-2.63	-1.36
56cc	<i>Nuttallides</i>	540.00	-2.45	-1.06
60cc	<i>Oridorsalis</i>	578.80	-2.95	-1.16
60cc	<i>Nuttallides</i>	578.80	-2.70	-0.40
60cc	<i>Stilostomella</i>	578.80	-2.37	-0.93
61cc	<i>Oridorsalis</i>	586.90	-3.17	-0.57
61cc	<i>Oridorsalis</i>	588.40	-3.56	-1.22
61cc	<i>Nuttallides</i>	588.40	-3.35	-0.67
61cc	<i>Cibicidoides</i>	588.40	-3.72	-0.34
62-3, 60-63	<i>Nuttallides</i>	601.70	-2.61	-0.49
63-1, 139-141	<i>N. Trumpeyi</i>	609.19	-3.14	-0.55
66-3, 57-59	<i>N. Trumpeyi</i>	640.37	-2.40	0.18
68-1, 29-31	<i>N. Trumpeyi</i>	656.49	-3.01	0.35

**Table 7 (continued).**

Core, section, interval (cm)	Species	Depth (m)	$\delta^{18}\text{O}$ (PDB)	$\delta^{13}\text{C}$ (PDB)
105-647A-68-3, 74-76	<i>Oridorsalis</i>	659.94	-3.01	-0.60
68-3, 74-76	<i>N. Trumpeyi</i>	659.94	-2.78	0.25
68-3, 74-77	<i>Cibicidoides</i>	659.94	-3.26	0.29
30-1, 51-53	Bulk	279.91	-0.32	0.87
36-4, 42-44	Bulk	342.12	-1.39	-4.32
36-4, 42-44	Bulk	342.12	-1.29	-3.78
38-6, 67-69	Bulk	364.57	-2.60	-6.23
43-4, 25-27	Bulk	409.55	-3.09	-2.54
46-5, 111-113	Bulk	440.91	-3.40	-1.69
48-1, 7-9	Bulk	453.27	-3.57	-3.95
50-4, 32-34	Bulk	477.32	-2.11	-2.06
51-4, 68-70	Bulk	487.28	-1.38	-5.68
51-4, 68-70	Bulk	487.28	-1.99	-6.03
51-6, 83-83	Bulk	490.43	-1.45	-0.43
52-2, 10-12	Bulk	493.40	-2.89	-0.16
53-4, 79-81	Bulk	506.45	-1.47	-7.04

values suggest somewhat deeper burial diagenesis, as discussed below.

#### Bulk Sample Analyses

Stable isotope analyses were also conducted on a limited number of bulk samples. The oxygen isotopic composition of these samples shows considerable variation with depth, similar to that observed in the benthic-foraminiferal isotope record. The heaviest measured values occur in the lower Oligocene part of the sequence, where a single sample at 279.91 mbsf yielded a  $\delta^{18}\text{O}$  value of  $-0.32\text{\textperthousand}$ . The gradual depletion in bulk-sample oxygen isotope composition occurs from 300 to 400 msbf, with a trend similar to that recorded by the benthic foraminifers. Below 400 msbf, bulk-sample  $\delta^{18}\text{O}$  values vary between  $-3.57$  and  $-1.38\text{\textperthousand}$ , with the lighter values generally corresponding to the lighter benthic foraminiferal values. The correspondence between bulk-sample and benthic foraminifers records suggest that burial diagenesis affected the isotopic composition of the benthics, as well as the bulk carbonate (mainly fine fraction).

A simple model can be constructed that constrains the timing and conditions under which burial diagenesis here may have occurred. Using a slightly modified equation of Killingley (1983) and assuming a closed system, a set of simple equations can be derived to calculate the "final" composition of the recrystallized carbonate ( $\delta^{18}\text{O}_{r-f}$ ), as well as the overall effect on the bulk-carbonate composition ( $\delta^{18}\text{O}_{b-f}$ ), if the initial composition of the carbonate is known or can be estimated.

$$\delta^{18}\text{O}_{r-f} = M_C R / [\delta^{18}\text{O}_{b-i} + 10^3(1 - \alpha T)] + M_{iw} \delta^{18}\text{O}_{iw} \quad (1)$$

$$(M_{iw} + M_C) \alpha T.$$

$$\delta^{18}\text{O}_{b-f} = R \delta^{18}\text{O}_{r-f} + (1 - R) \delta^{18}\text{O}_{b-i}. \quad (2)$$

In these equations,  $\delta^{18}\text{O}_{b-i}$  is the initial composition of the bulk carbonate and  $R$  is the percentage of the bulk carbonate that undergoes dissolution and/or recrystallization. The initial composition of the interstitial waters,  $\delta^{18}\text{O}_{iw}$ , is derived from analyses of Zachos and Cederberg (Fig. 12A and this volume), which show a  $-0.88\text{\textperthousand}$  (SMOW)/100 m gradient at this site. The initial bottom-water oxygen isotopic composition is assumed to be  $0\text{\textperthousand}$  (SMOW). The number of moles of carbonate,  $M_C$ , and interstitial water,  $M_{iw}$  at the site of recrystallization, were determined using wet bulk density (WBD) (Srivastava, Arthur, et al., 1987) and percent carbonate (%  $\text{CaCO}_3$ ) data (Fig. 1; Table 1) in the following equations:

$$M_C = [(WBD - P [1.01 g]) \% \text{ (fraction) } CO_3]/100 \text{ g}, \quad (3)$$

$$M_{iw} = [P (1.01 g)]/18 \text{ g (closed-system formulation)}, \quad (4)$$

$$P = P_o e^{-cz}, \quad (5)$$

where  $P$ , porosity at the time of diagenesis, was estimated using a compaction equation (5) in which  $P_o$  is the original porosity at the time of deposition,  $c$  is the compaction factor, which is a function of the major sediment components, and  $z$  is the depth of burial. Model calculations were performed assuming that the sediment is 40% carbonate by weight. The fractionation factor  $\alpha$ , for calcite-water at a given temperature, was obtained from Friedman and O'Neil (1977) and  $T$ , the ambient temperature of the system at the time of diagenesis, was determined using the thermal gradient for this region of  $7.4^\circ\text{C}/100 \text{ m}$  (Srivastava, Arthur, et al., 1987). The initial temperature was assumed to be near that of bottom waters ( $< 10^\circ\text{C}$  for late Eocene to present).

The model was run for varying degrees of recrystallization (Fig. 12B) using two different initial  $\delta^{18}\text{O}$  compositions for the bulk carbonate. The first model was run assuming a modern  $\delta^{18}\text{O}$  composition for bulk carbonate (+0.5 in Fig. 12B), with an initial temperature of  $5^\circ\text{C}$  for bottom water. The second run was conducted assuming (1) that the bulk-carbonate composition is equal to that of nannofossil-carbonate, which makes up more than 95% of the carbonate, and (2) that the isotopic composition of the nannofossils is equal to that of carbonate secreted in isotopic equilibrium at ambient surface-water temperatures at the time of formation in the Eocene (-1.0 in Fig. 12B). There are few available temperature estimates for Eocene surface waters in this region, but we assumed a temperature of  $16^\circ\text{C}$ , based on temperature estimates for surface waters in other early to late Eocene regions of the North Atlantic (Miller et al., 1987).

This model predicts the expected range of isotopic compositions that could be obtained theoretically for variable amounts of recrystallization and a range in burial depths. If we compare the model curves with data from Site 647, we discover that less than 50% of the original carbonate in bulk samples at 400 mbsf needed to recrystallize in equilibrium with interstitial waters to produce the observed  $\delta^{18}\text{O}$  composition of  $-4.0\text{\textperthousand}$ . The same oxygen isotopic composition at shallower buried depths would require a greater percentage of the carbonate to have undergone recrystallization. If we assume that most of the diagenesis occurred between 300 and 400 mbsf, from 50% to 75% of the original carbonate must have dissolved and reprecipitated as cement to obtain  $\delta^{18}\text{O}$  values of  $-4.0\text{\textperthousand}$ .

This approach assumes that most of the diagenesis occurred at some threshold depth at which carbonate instability was reached instantaneously. Although this probably is unrealistic, the model does help to constrain the conditions under which diagenesis occurred.

Whereas the  $\delta^{18}\text{O}$  trends for bulk samples are easily explained in terms of burial diagenesis, the  $\delta^{13}\text{C}$  record requires a more complicated interpretation. Most of the samples have  $\delta^{13}\text{C}$  values of  $-2.0$  to  $1.0\text{\textperthousand}$ , but extremely light values in the range of  $-7.0$  to  $-6.0\text{\textperthousand}$  were recorded for a number of bulk samples from discrete intervals. The more negative  $\delta^{13}\text{C}$  values occur in intervals where high concentrations of siderite and rhodochrosite were observed. Both minerals tend to precipitate at the boundaries of reducing zones, where an ample supply of Fe, Mn, and carbonate ions are available. The carbon isotopic composition of pore-water total dissolved carbonate in OC-rich sediments is more negative than that in average seawater, mainly due to the addition of isotopically light  $CO_2$  derived from decaying organic matter. As a result, authigenic carbonate minerals formed during early diagenesis would be isotopically light,

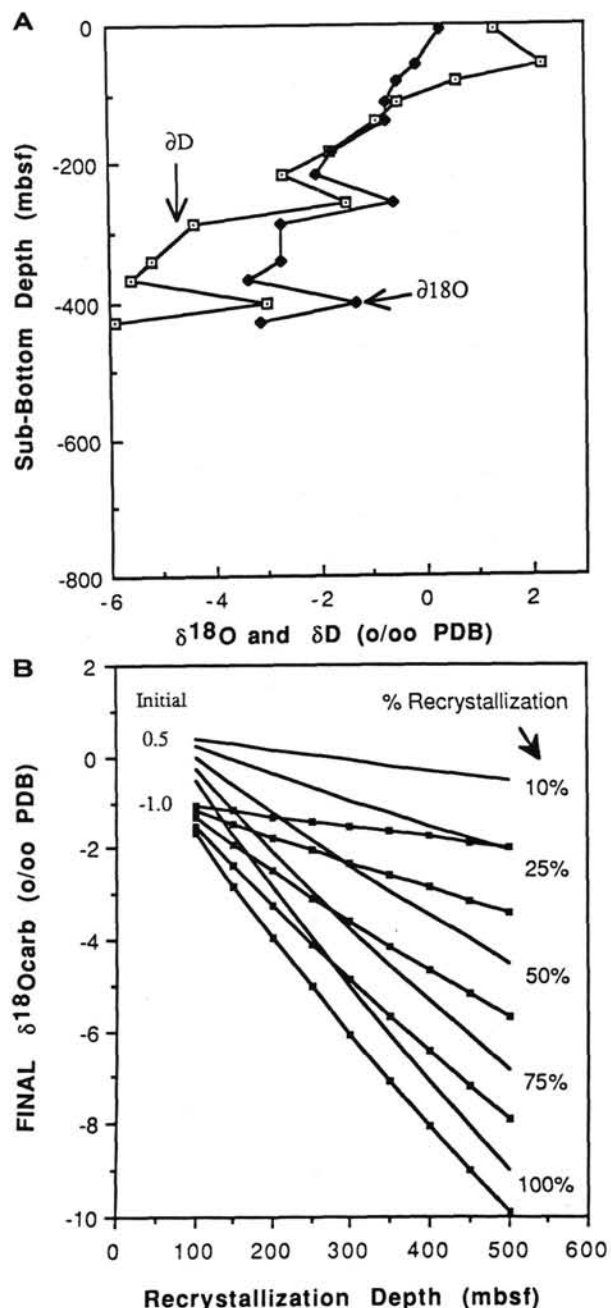


Figure 12. A. Trends in oxygen and deuterium isotopic composition of interstitial waters with depth in Hole 647A (from Zachos and Cederberg, this volume) showing downhole decrease. B. Results of a diagenetic model (see text for details) that predicts the  $\delta^{18}\text{O}$  of calcite recrystallized at a given depth with a geothermal gradient of  $7.4^\circ\text{C}/100 \text{ m}$ . The two families of curves represent alteration of two different starting compositions for bulk carbonate (+0.5‰ and -1.0‰, PDB, respectively) and different proportions of calcite recrystallized at a given sub-bottom depth.

compared to biogenic carbonate. This conclusion is discussed later in the context of the depositional regime that prevailed at Site 647 during the Eocene/Oligocene.

## DISCUSSION

There are several anomalous aspects to the geochemistry of the hemipelagic sequence at Site 647. In particular, we noted in-

ervals of high Fe, Mn,  $P_2O_5$ , and associated elements, which are related to authigenic carbonate and apatite precipitates. The origin of these and other geochemical characteristics of the Eocene-Oligocene sequence is discussed below.

The diagenetic precipitation of Fe and Mn-carbonate minerals in Tertiary hemipelagic sediments is not that unusual. Disseminated and nodular siderite has been described from the late Paleogene and Neogene from a number of DSDP sites in the western North Atlantic (Sites 102, 104—Lancelot et al., 1972; Site 533—Matsumoto, 1983; Site 603—von Rad and Botz, 1986) and Pacific (Middle America Trench: Wada et al., 1982; Japan Trench: Matsumoto and Matsuhisa, 1986). These occurrences are in hemipelagic sequences characterized by high rates of deposition and preservation of sufficient organic matter to promote total consumption of dissolved sulfate by bacterial sulfate reduction, followed by strong methanogenesis (e.g., von Rad and Botz, 1986; Matsumoto, 1983; Claypool and Kaplan, 1984). Dolomite occurs in many of the same sediments that contain siderite. Matsumoto (1983) argued that dolomite precipitation occurs at relatively shallow depths in the Blake-Bahama Outer Ridge (Site 533) during late stages of sulfate reduction and early methanogenesis, followed by authigenic siderite at greater depth within the sediment. Similar results were obtained for Japan Trench sediments using oxygen and carbon isotope constraints (e.g., Irwin et al., 1977; Okada, 1980; Wada and Okada, 1983; Matsumoto and Matsuhisa, 1986).

The growth of Fe and Mn authigenic phases clearly requires the elevated alkalinity,  $CO_3^{2-}$  and  $TCO_2$  concentrations that accompany extensive degradation of organic matter, as well as a source of soluble Fe and Mn that are released under low redox conditions. Siderite precipitation also implies available Fe in excess of that necessary to form pyrite from the dissolved sulfide that results from bacterial sulfate reduction.

### Timing and Geochemical Conditions of Precipitation

The carbon and oxygen isotopic compositions of discrete carbonate nodules provide constraints on the timing of precipitation and origin of the authigenic Fe-Mn carbonates (e.g., Irwin et al., 1977; Gautier, 1985). Carbon isotopic compositions of the homogenized nodules (no attempt was made to examine possible zonation of nodules in this study) range between  $-2$  and  $-6\text{\textperthousand}$  (PDB). These values indicate that carbonate ion was drawn from a somewhat  $^{13}C$ -depleted pore-water carbon reservoir that resulted from oxidation of organic matter. Pore-water dissolved sulfate concentrations (Zachos and Cederberg, this volume) reach a minimum at 500 mbsf but do not decrease below about 13 mmol/L. Thus, sufficient reactive organic matter may have been available to promote consumption of initial dissolved oxygen and partial bacterial sulfate reduction, but methanogenesis may never have occurred. This was confirmed when monitoring of head-space gas during drilling at Site 647 detected no methane (Srivastava, Arthur, et al., 1987). Present sedimentary organic carbon contents are generally low, ranging from 0.2 to 0.5 wt% (Fig. 1). Because there was insufficient pore water with which to determine total dissolved inorganic carbon (TDC) or  $\delta^{13}C_{TDC}$ , we must estimate the  $\delta^{13}C_{TDC}$  on the basis of a  $\Delta SO_4^{2-}$  of about 15 mmol/L, assuming a  $\Delta SO_4^{2-}$ :  $HCO_3^-$  ratio of 1:2 (TDC increases in proportion to the sulfate decrease) during sulfate reduction and a  $-22\text{\textperthousand}$   $\delta^{13}C$  value for the largely marine organic matter undergoing oxidation. The calculated minimum pore-water  $\delta^{13}C_{TDC}$  value is about  $-20\text{\textperthousand}$ . Therefore, it is likely that the authigenic Fe-Mn carbonates precipitated during early diagenesis, before the main phase of bacterial sulfate reduction, or that the Fe-Mn carbonates are a partial replacement of preexisting calcium carbonate having initially heavier  $\delta^{13}C$ . The  $\delta^{18}O$  values of the nodular carbonates have a range of  $-1.30$  to  $-3.50\text{\textperthousand}$  (PBD) (Table 7). Using these

data to estimate temperatures of formation is difficult because oxygen-isotopic fractionation factors between water and siderite and phosphoric acid and siderite have only recently been experimentally determined (Carothers et al., 1988). The isotope fractionation effects of bonding of different metals with carbonate also have been estimated theoretically (Tarutani et al., 1969), and Sharma and Clayton (1965) reported the fractionation factor for rhodochrosites. Siderite should be about  $0.9\text{\textperthousand}$  to  $1.5\text{\textperthousand}$  heavier than coexisting calcite; whereas, rhodochrosite should be similar in composition to coprecipitated calcite. Using an assumed  $\delta^{18}O$  of Eocene seawater of  $-1.2\text{\textperthousand}$  (SMOW; pre-glacial), the estimated temperature range for siderite or rhodochrosite precipitation would be  $28^\circ$  to  $30^\circ\text{C}$ . Estimated bottom-water temperatures for the Atlantic Ocean during the mid-to-late Eocene range from  $8^\circ$  to  $12^\circ\text{C}$  (e.g., Shackleton, 1986; Miller et al., 1985), so that the  $\delta^{18}O$  data from the nodules suggest precipitation following some burial. Pore water  $\delta^{18}O$  at Site 647 (below about 300 mbsf) is presently about  $-3\text{\textperthousand}$  (SMOW; Zachos and Cederberg, this volume), which at *in-situ* temperatures of about  $35^\circ\text{C}$ , would produce siderite with a  $\delta^{18}O$  of about  $-5$  to  $-6\text{\textperthousand}$  (PDB). Therefore, the authigenic carbonate nodules formed at shallow depths of burial, perhaps no more than 100 to 200 m. Separation of pure mineral phases for isotopic studies was not possible, and one must keep in mind that we analyzed only mixtures, which precludes a more detailed interpretation of the  $\delta^{18}O$  values at this time.

Whereas previous research suggests an association of Fe- and Mn-carbonates with methanogenesis, our data from Site 647 indicate that such geochemical conditions are not a prerequisite (see also Suess, 1979). However, there is little doubt that such mineralization is more extensive in methane-associated settings, which may be true for anoxic dolomites as well (e.g., Kelts and McKenzie, 1982).

One can see by inspection that the highest Fe/Al ratios (Fig. 13) occur in the intervals of documented increase in the relative abundance of concretions or nodules and that some, but not all, of the high Fe/Al ratios correspond to intervals of higher Fe/Mn as well. We would expect redox separation of Fe from Mn, as it has been described from many modern environments (e.g., Froelich et al., 1979; Li, 1982). Because of the effect of dilution of Al by higher carbonate contents and because both Fe and Mn are incorporated in the carbonate phases in varying amounts, we have also plotted the moving correlation coefficient for the relationship between Fe/Al and Fe/Mn ratios in Figure 13. The correlation coefficients indicate variation mainly between intervals of strong negative ( $r = -0.65$ ) and relatively, strong positive ( $r = 0.60$ ) correlation. Over much of the sequence (260–415 mbsf; 465–485 mbsf) variations in Fe and Mn concentrations may be positively correlated, even though the Fe/Mn ratio varies considerably. A few intervals of generally positive Fe/Al—Fe/Mn correlation (415–465 mbsf and  $>500$  mbsf) are mainly characterized by lower concentrations of Fe and Mn overall. These are most likely the “source” intervals from which the necessary “excess” Fe, and particularly excess Mn, migrated for precipitation as authigenic phases. Coarse-grained, initially more carbonate-rich beds may have catalyzed precipitation. We were unable to confirm this by examining the cores, but the need for some sort of coarser-grained nucleation site was postulated by Pederson and Price (1982) for more recent nonmethane-associated manganese-carbonates of the Panama Basin. Bohrmann and Thiede (this volume) examined Fe-Mn carbonates from deeper in the sequence in Hole 647A (cores 105–647A-62 through -71) and found that they commonly occur as precompaction burrow-filling cements and that Mn is more important than Fe in cation substitution into the authigenic carbonate phases. Iron concentrations are higher on average in the lower part of lithologic Unit III that we analyzed, and in nodu-

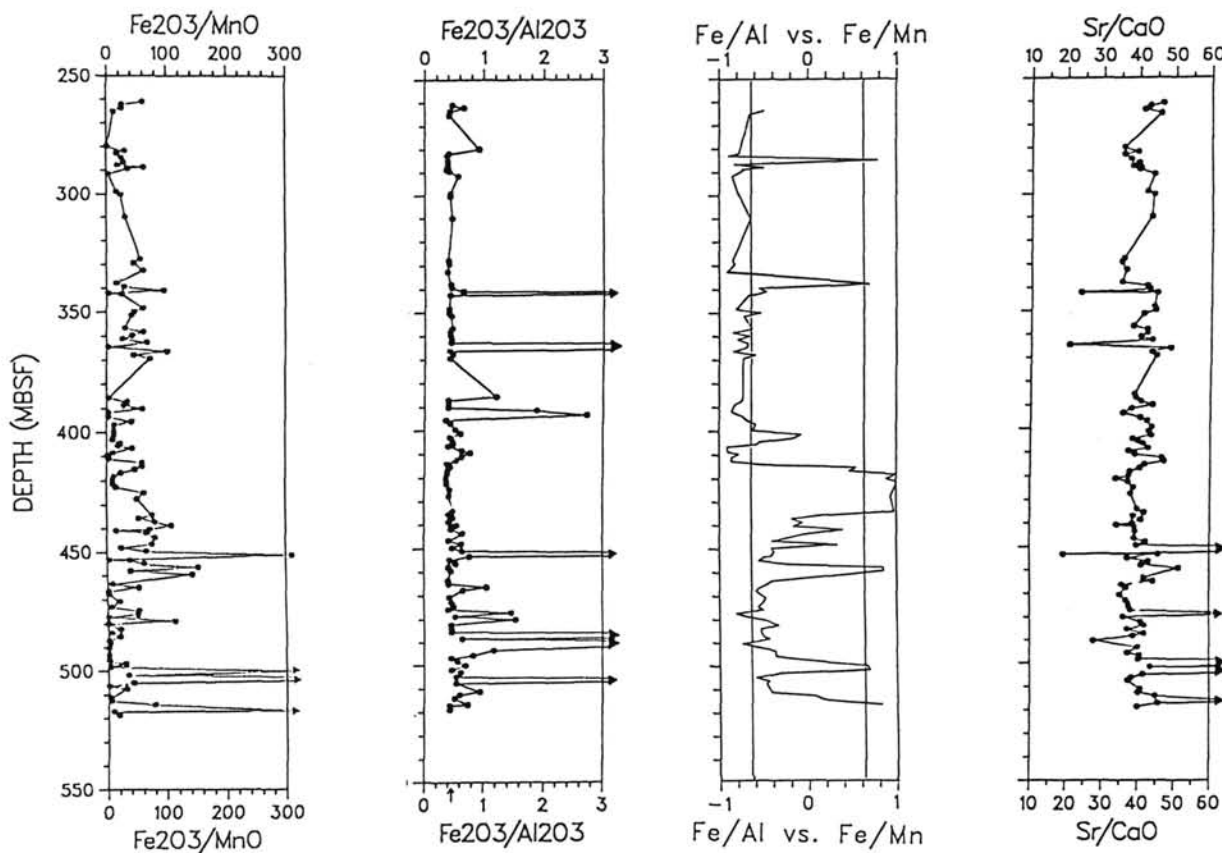


Figure 13.  $\text{Fe}_2\text{O}_3/\text{MnO}$ ,  $\text{Fe}_2\text{O}_3/\text{Al}_2\text{O}_3$ , moving correlation coefficients of  $\text{Fe}/\text{Al}$  vs.  $\text{Fe}/\text{Mn}$  and  $\text{Sr}/\text{CaO}$  ( $\times 10^{-4}$ ) for lithologic Unit IIIc, Hole 647A.

lar or concretionary horizons in general, than they are in the Unit IV samples analyzed by Bohrmann and Thiede (this volume).

Although those authors hypothesized that possible hydrothermal oxyhydroxides were a source of excess Mn and Fe for lithologic Unit IV, our geochemical data for Unit III do not require a significant hydrothermal flux. The average or baseline  $\text{Fe}/\text{Al}$  ratio (Fig. 13—see arrow) is similar to or only slightly Fe-enriched, compared to that in abyssal red clay of the recent North Atlantic (V26-157; Table 3). However, the average Mn concentration in "background" samples at Site 647 (Table 3) is higher by a factor of four on a carbonate-free basis and the Mn/Al ratio higher by a factor of five. This might suggest some additional hydrothermal flux to the site, and other indications of this might appear in the geochemical data. For example, Figure 14 is a comparison of the geochemistry (carbonate-free) of 99 background (nonconcretionary, good correspondence between CC as  $\text{CaCO}_3$  and Ca as  $\text{CaCO}_3$ ) Site 647 samples with that of modern northern Atlantic abyssal red clay. This diagram illustrates that Mn, Co, Ca, and Ba are somewhat enriched at Site 647, which could also be related to a minor hydrothermal detritus flux (see below). Phosphate is also enriched in some of the concretionary horizons (Figs. 3 and 15) and occurs as a discrete authigenic apatite phase. The origin of the P enrichments is probably related to desorption of P from Fe-Mn oxyhydroxides during chemical reduction and dissolution of those phases (e.g., Froelich et al., 1979). Sr is relatively enriched in carbonate-phosphatic nodules (Figs. 13 and 15), but not in the Fe- and Mn-rich carbonates. Because the  $\text{Sr}/\text{Ca}$  ratio in pore waters increases with depth (Zachos and Cederberg, this volume), the in-

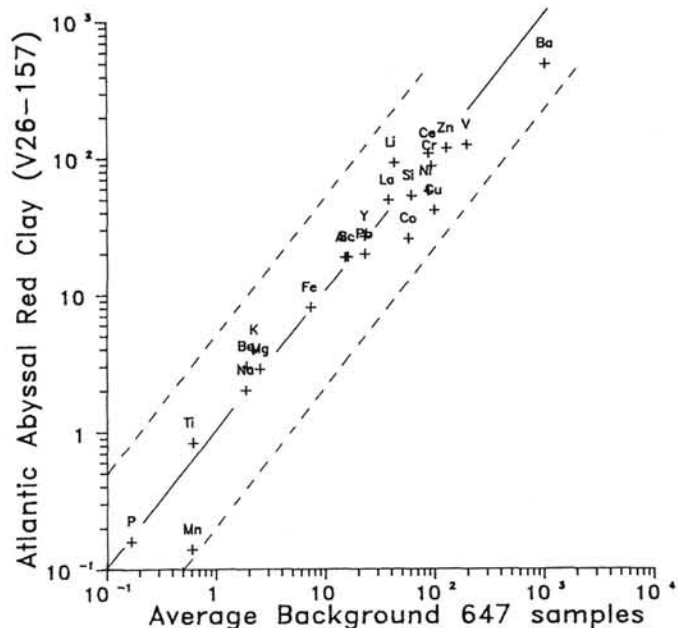


Figure 14. Plot comparing elemental concentrations of average "background" Site 647 samples ( $n = 99$ ) on carbonate-free basis with those for Atlantic abyssal red clay (V26-157). Solid line represents a 1:1 correspondence.

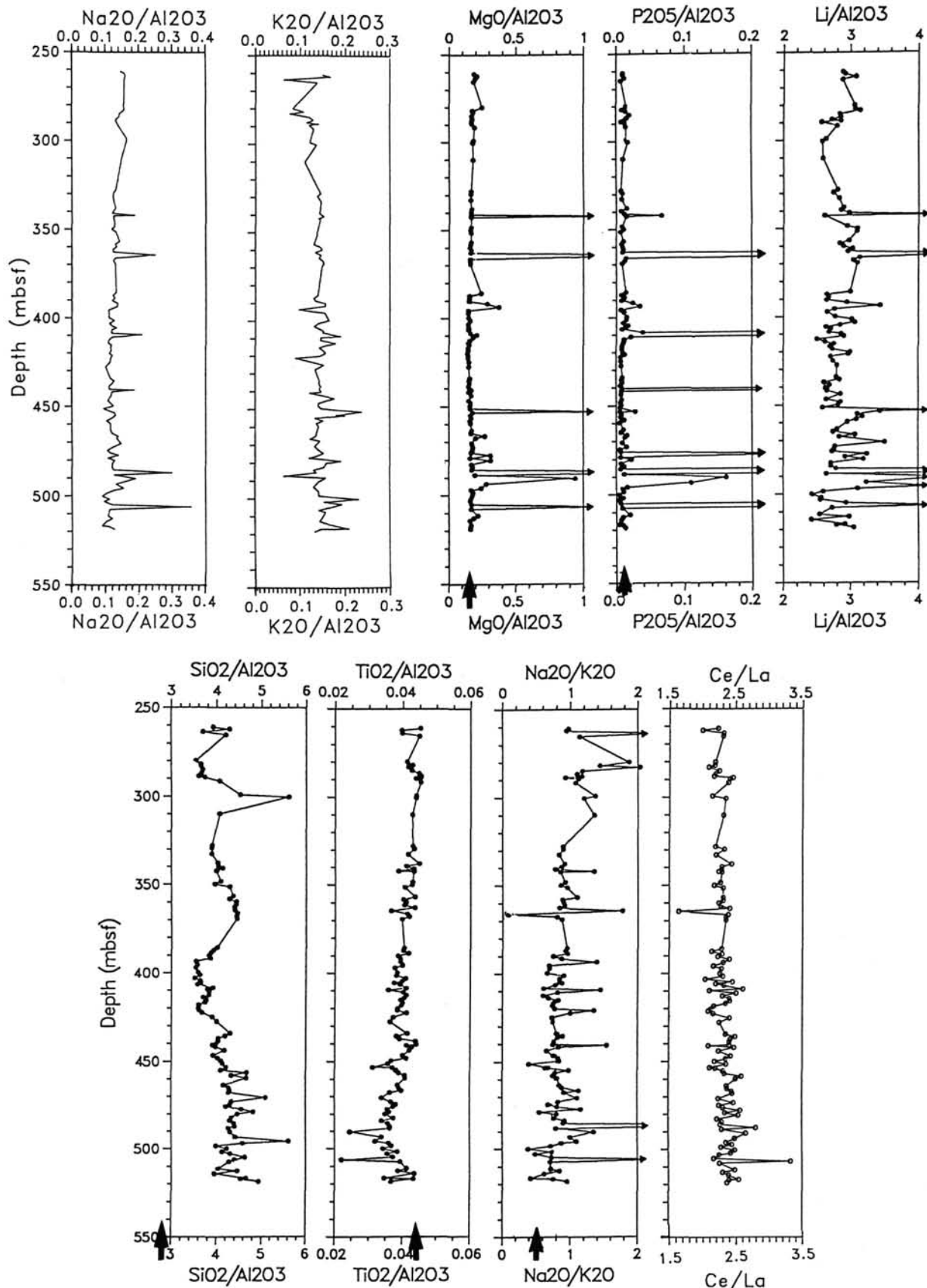


Figure 15. A.  $\text{SiO}_2/\text{Al}_2\text{O}_3$ ,  $\text{TiO}_2/\text{Al}_2\text{O}_3$ ,  $\text{Na}_2\text{O}/\text{K}_2\text{O}$ , and  $\text{Ce}/\text{La}$  ratios plotted downhole for lithologic Unit IIIC of Hole 647; arrows on bottom axis denote average Atlantic red clay (V26-157) values. B.  $\text{Na}_2\text{O}/\text{Al}_2\text{O}_3$ ,  $\text{K}_2\text{O}/\text{Al}_2\text{O}_3$ ,  $\text{MgO}/\text{Al}_2\text{O}_3$ ,  $\text{P}_2\text{O}_5/\text{Al}_2\text{O}_3$ , and  $\text{Li}/\text{Al}_2\text{O}_3$  values for lithologic Unit IIIC of Hole 647A plotted downcore.

creased Sr/Ca ratio in some nodules may indicate later-stage precipitation.

#### Other Geochemical Signals

Major-element aluminum ratios (Fig. 15) overall exhibit little change from the base to the top of the sequence. However, there are several important trends to note. The Si/Al ratio varies from above 4 in the middle Eocene (430–525 mbsf) to a low of about 3.5 at the middle/upper Eocene boundary and fluctuates somewhat above that level to a high centered at about 310 mbsf. For this study our samples were collected from well below the lower Oligocene biogenic opal-rich sequence (above 240 mbsf). However, it is likely that the Si/Al variations reflect changes in the original amounts of biogenic silica in the Eocene, suggesting that the mid-middle Eocene and latest Eocene were times of higher surface-water opal production. Our data confirm and amplify the conclusions of Bohrmann and Stein (this volume) and Nielsen et al. (this volume), who used visual and geochemical and X-ray mineralogical techniques, respectively. On the basis of these studies, most of the original opal may have dissolved and reprecipitated as authigenic smectite or opal CT. The Mg/Al ratio concentration is also relatively constant (Fig. 15), with the exception of high Mg spikes that are associated with Fe-Mn carbonate horizons. Mg probably was substituted in the lattice of these carbonates. However, no discrete dolomite was detected in our X-ray mineralogical studies.

Ce/La and Li/Al ratios decrease gradually upsection (Fig. 15). This is interesting in light of the possible decreasing importance of a minor hydrothermal component. However, Li concentrations in pore waters also increase downhole (Zachos and Cederberg, this volume), so that the prevalence of authigenic smectite formation in the lower part of Unit III and in Unit IV (Bohrmann and Stein; Nielsen et al., this volume) might explain the higher sediment Li/Al ratios. Concentrations of Li and REEs, as well as those of Mn, V, Zn, Ni, and Cu are relatively enriched in comparison to Atlantic red clays (Fig. 14). Higher Ba and Co concentrations would result from somewhat higher productivity and organic-associated fluxes in the Eocene at Site 647 in comparison to the central North Atlantic Ocean today. Biogenic detritus, particularly marine particulate organic matter, incorporates or absorbs trace elements (e.g., Boström et al., 1974; Collier and Edmond, 1974) as do fine-grained clay minerals (e.g., Balistrieri et al., 1981). At this point, it is difficult to separate the potential variations in sediment adsorption capacity in this clay-rich sediment (e.g., Balistrieri and Murray, 1984) from potential hydrothermal sources.

Finally, Ti/Al, Na/Al, and Na/K ratios increase significantly above 320 mbsf (uppermost Eocene). This may reflect an increase in average sediment grain-size (Nielsen et al., this volume) and increasing feldspar and detrital clay proportions as opposed to smectite, related to climate deterioration and an increase in bottom-current strength near the Eocene/Oligocene boundary.

#### CONCLUSIONS

The geochemistry of background sediment of lithologic Unit III at 647 of middle Eocene to lower Oligocene age is remarkably constant and similar to that of modern Atlantic red clay, which has a distinctly terrigenous geochemical composition. Nonetheless, the high sedimentation rates (average 36 m/m.y.) over this interval (260–515 mbsf) led to some initial preservation of organic matter and to anoxic early diagenesis and sulfate reduction. Sulfate reduction led to reduction of Fe and Mn oxyhydroxides, to increased pore-water alkalinity and TCO<sub>2</sub> and to higher pore-water phosphate concentrations, all of which allowed precipitation of authigenic Fe-Mn carbonates and apatite at a number of horizons in the sequence.

Because of this early diagenesis, there may be no opportunity to unravel paleoenvironment changes from the stable isotopic composition of biogenic carbonate phases. In particular, although benthic foraminiferal preservation visually is moderate-to-good over most of the sequence, both oxygen and carbon isotopic compositions indicate significant burial diagenesis. Such pronounced alteration was unexpected in such shallowly buried, relatively clay-rich and organic carbon-poor sediments.

The geochemical data suggest that there was a possible minor hydrothermal component to the sediment, the proportion of which wanes through time and distance from the potential source. Concentrations of Mn, Co, Cu, and Ba are higher than expected for a purely terrigenous source, and the relatively high Li/Al and Ce/La ratios may indicate a hydrothermal component as well. Si/Al ratios are high in upper middle Eocene and upper Eocene portions of the sequence, confirming biogenic opal flux to the seafloor at those times, which are inferred to have been characterized by higher paleoproductivity. Average Na/K ratios are constant through the sequence, except near the top of Unit IIIC, where the ratio increases significantly. This occurs in conjunction with an increase in the relative proportion of silt-sized sediment and in feldspar concentrations, which suggest that the feldspar is a more sodium-rich variety.

Future more-detailed geochemical studies and comparison of units above and below Unit IIIC will help elucidate the question of the importance of a hydrothermal source for some sedimentary components.

#### ACKNOWLEDGMENTS

We would like to acknowledge the help of the crew of the *JOIDES Resolution*, without whose efforts these samples would not have been available. We appreciate the efforts of Rhonda Kenny in preparation of this manuscript. Part of this study was funded by JOI-USSAC Contract 76322 to MAA.

#### REFERENCES

- Addy, S. K., 1979. Rare earth element patterns in manganese nodules and micronodules from northwest Atlantic. *Geochim. Cosmochim. Acta*, 43:1105–1115.
- Arthur, M. A., Hagerty, S., Dean, W. E., Claypool, G. E., Daws, T. A., McManaman, D., Meyers, P. A., and Dunham, K., 1987. A geochemical note: comparison of techniques for obtaining CaCO<sub>3</sub>, organic carbon, and total nitrogen in limestones and shales. *In* van Hinte, J. E., Wise, S. W., Jr., et al., *Init. Repts. DSDP*, 92: Washington (U.S. Govt. Printing Office), 1263–1268.
- Baedeker, P. (Ed.), 1987. *Methods for Geochemical Analysis*: Washington (U.S. Govt. Printing Office), USGS Bull. 1770.
- Balistrieri, L., Brewer, P. G., and Murray, J. W., 1981. Scavenging residence times of trace metals and surface chemistry of sinking particles in the deep ocean. *Deep-Sea Res.*, 28(A):101–121.
- Balistrieri, L. S., and Murray, J. W., 1984. Marine scavenging: trace metal adsorption by interfacial sediment from MANOP Site H. *Geochim. Cosmochim. Acta*, 48:921–929.
- Bischoff, J. L., Heath, G. R., and Leinen, M., 1979. Geochemistry of deep-sea sediments from the Pacific manganese nodule province: DOMES Sites A, B, and C. *In* Bischoff, J. L., and Piper, D. Z. (Eds.), *Marine Geology and Oceanography of the Pacific Manganese Nodule Province*: New York (Plenum Press), Mar. Sci. Ser., 9: 397–436.
- Boersma, A., Premoli-Silva, I., and Shackleton, N. J., 1987. Atlantic Eocene planktonic foraminiferal paleohydrographic indicators and stable isotope paleoceanography. *Paleoceanography*, 2:287–331.
- Boström, K., Joensuu, O., and Broihm, I., 1974. Plankton: its composition and its significance as a source of pelagic sediments. *Chem. Geol.*, 14:255–271.
- Boström, K., and Peterson, M.N.A., 1969. The origin of aluminum-poor ferromanganese sediments in areas of high heat flow on the East Pacific Rise. *Mar. Geol.*, 7:427–447.
- Carothers, W. W., Adami, L. H., and Rosenbauer, R. J., 1988. Experimental oxygen-isotope fractionation between siderite-water and phosphoric acid liberated CO<sub>2</sub>-siderite. *Geochim. Cosmochim. Acta*, 52: 2445–2450.

- Chester, R., and Aston, S. R., 1976. The geochemistry of deep-sea sediments. In Riley, J. P., and Chester, R. (Eds.), *Chemical Oceanography*: New York (Academic Press), 6:281-390.
- Claypool, G. E., and Kaplan, I. R., 1974. The origin and distribution of methane in marine sediments. In Kaplan, I. R. (Ed.), *Natural Gases in Marine Sediments*: New York (Plenum Press), 99-139.
- Collier, R., and Edmond, J., 1984. The trace element geochemistry of marine biogenic particulate matter. *Prog. Oceanogr.*, 13:113-199.
- Dean, W. E., and Pahrduhn, N. L., 1984. Inorganic geochemistry of sediments and rocks recovered from the southern Angola Basin and adjacent Walvis Ridge, Sites 530 and 532, Deep Sea Drilling Project Leg 75. In Hay, W. W., Sibuet, J.-C., et al., *Init. Repts. DSDP*, 75 (Pt. 2): Washington (U.S. Govt. Printing Office), 923-958.
- Friedman, I., and O'Neil, J. R., 1977. Compilation of stable isotope fractionation factors of geochemical interest. In Fleischer, M. (Ed.), *Data of Geochemistry*. U.S. Geol. Surv. Prof. Pap., 440KK.
- Froelich, P. N., Klinkhammer, G. P., Bender, M. L., Luedtke, N. A., Heath, G. R., Cullen, D., Dauphin, P., Hammond, D., Hartman, B., and Maynard, V., 1979. Early oxidation of organic matter in pelagic sediments of the eastern equatorial Atlantic: suboxic diagenesis. *Geochim. Cosmochim. Acta*, 43:1075-1090.
- Goldschmidt, V. M., 1958. *Geochemistry*: London (Oxford Univ. Press).
- Huffman, E. W.D., 1977. Performance of a new automatic carbon dioxide coulometer. *Microchem. J.*, 22:567-573.
- Irwin, H., Curtis, C. D., and Coleman, M., 1977. Isotopic evidence for source of diagenetic carbonates formed during burial of organic-rich sediments. *Nature*, 269:209-213.
- Keigwin, L., 1980. Paleoceanographic change in the Pacific at the Eocene/Oligocene boundary. *Nature*, 277:722-725.
- Keigwin, L., and Corliss, B., 1986. Stable isotopes in Eocene/Oligocene foraminifera. *Geol. Soc. Am. Bull.*, 103:197-236.
- Kelts, K., and McKenzie, J. A., 1982. Diagenetic dolomite formation in Quaternary anoxic diatomaceous muds of Deep Sea Drilling Project Leg 64, Gulf of California. In Curry, J., Moore, D. G., et al., *Init. Repts. DSDP*, 64 (Pt. 2): Washington (U.S. Govt. Printing Office), 553-570.
- Killingly, J., 1983. Effects of diagenetic recrystallization on  $^{18}\text{O}/^{16}\text{O}$  values of deep-sea sediments. *Nature*, 301:594-597.
- Klovan, J. E., and Miesch, A. T., 1976. Extended CABFAC QMODEL computer programs for Q-mode factor analysis of compositional data. *Comp. Geosci.*, 1:161-178.
- Lancelot, Y., Hathaway, J., and Hollister, C. D., 1972. Lithology of sediments from the western North Atlantic, Leg 11, Deep Sea Drilling Project. In Hollister, C. D., Ewing, J., et al., *Init. Repts. DSDP*, 11: Washington (U.S. Govt. Printing Office), 901-949.
- Li, Y.-H., 1982. Interelement relationship in abyssal Pacific ferromanganese nodules and associated pelagic sediments. *Geochim. Cosmochim. Acta*, 46:1053-1060.
- McCorkle, D. C., 1987. Stable carbon isotopes in deep-sea pore waters: modern geochemistry and paleoceanographic implications [Ph.D. diss.]. Univ. of Washington, Seattle.
- Miller, K. G., Curry, W. B., Ostermann, D. R., 1985. Late Paleogene (Eocene to Oligocene) benthic foraminiferal oceanography of the Goban Spur region. In de Graciansky, P. C., Poag, C. W., et al., *Init. Repts. DSDP*, 80: Washington (U.S. Govt. Printing Office), 1089-1106.
- Miller, K. G., Fairbanks, R. G., and Mountain, G. S., 1987. Tertiary oxygen isotope synthesis, sea-level history, and continental margin erosion. *Paleoceanography*, 1:1-19.
- Matsumoto, R., 1983. Mineralogy and geochemistry of carbonate diagenesis of the Pliocene and Pleistocene hemipelagic mud on the Blake Outer Ridge, Site 533, Leg 76. In Sheridan, R. E., Gradstein, F. M., et al., *Init. Repts. DSDP*, 76: Washington (U.S. Govt. Printing Office), 411-427.
- Matsumoto, R., and Matsuhisa, Y., 1986. Chemistry, carbon oxygen and isotope ratios, and origin of deep-sea carbonate at Sites 438, 439, and 584: inner slope of the Japan Trench. In Kagami, H., Kang, D. E., et al., *Init. Repts. DSDP*, 87: Washington (U.S. Govt. Printing Office), 669-678.
- Müller, P. S., and Suess, E., 1979. Productivity, sedimentation rate, and sedimentary organic carbon content in the oceans. *Deep-Sea Res.*, 26:1347-1362.
- Okada, H., 1980. Pebbles and carbonate nodules from Deep Sea Drilling Project Leg 56 cores. In Scientific Party, *Init. Repts. DSDP*, 56, 57(Pt. 2): Washington (U.S. Govt. Printing Office), 1089-1106.
- Pederson, T. F., and Price, N. B., 1982. The geochemistry of manganese carbonate in Panama Basin sediments. *Geochim. Cosmochim. Acta*, 46:59-68.
- Piper, D. Z., and Graef, P. A., 1974. Gold and rare-earth elements in sediments from the East Pacific Rise. *Mar. Geol.*, 17:287-297.
- Sayles, F. L., Ju, T. K., and Bowker, P. C., 1975. Chemistry of ferromanganese sediment of the Bauer Deep. *Geol. Soc. Am. Bull.*, 86: 1423-1431.
- Shackleton, N. J., 1986. Paleogene stable isotope events. *Palaeogeogr., Palaeoclimatol., Palaeocol.*, 57:91-102.
- Shackleton, N. J., and Kennett, J., 1975. Paleotemperature history of the Cenozoic and the initiation of Antarctic glaciation; oxygen and carbon isotope analysis in DSDP Sites 277, 279, 281. In Kennett, J. P., Houtz, R. E., et al., *Init. Repts. DSDP*, 29: Washington (U.S. Govt. Printing Office), 743-755.
- Sharma, T., and Clayton, R. N., 1965. Measurement of  $^{18}\text{O}/^{16}\text{O}$  ratios of total oxygen from carbonates. *Geochim. Cosmochim. Acta*, 29: 1347-1354.
- Suess, E., 1979. Mineral phases in anoxic sediments by microbial decomposition of organic matter. *Geochim. Cosmochim. Acta*, 43: 339-352.
- Tarutani, T., Clayton, R. N., and Mayeda, T. K., 1969. The effect of polymorphism and magnesium substitution on oxygen isotope fractionation between calcium carbonates and water. *Geochim. Cosmochim. Acta*, 33:987-996.
- von Rad, V., and Botz, R., 1986. Authigenic Fe-Mn carbonates in Cretaceous and Tertiary sediments of the continental rise off eastern North America, DSDP Site 603. In van Hinte, J., Wise, S., et al., *Init. Repts. DSDP*, 93: Washington (U.S. Govt. Printing Office), 1061-1078.
- Wada, H., Niitsuma, N., Nagasawa, K., and Okada, H., 1982. Deep-sea carbonate nodules from the Middle America Trench area off Mexico, Deep Sea Drilling Project Leg 66. In Watkins, J. S., Moore, J. C., et al., *Init. Repts. DSDP*, 66: Washington (U.S. Govt. Printing Office), 453-474.
- Wada, H., and Okada, H., 1983. Nature and origin of deep-sea carbonate nodules collected from the Japan Trench. In Watkins, J. S., and Drake, C. L. (Eds.), *Studies in Continental Margin Geology*. AAPG Mem., 34:661-672.
- Wedepohl, K. H., 1971. *Geochemistry*: New York (Holt, Rienhart, and Winston).

Date of initial receipt: 5 April 1988

Date of acceptance: 3 February 1989

Ms 105B-157